Fall 2017

Characterizing Basement Structures to Evaluate Their Influence on Overlaying Sedimentary Layers: Case Study of Three Fields in the Central Kansas Uplift

Muhammad S. Karim
Fort Hays State University, mskarim@mail.fhsu.edu

CHARACTERIZING BASEMENT STRUCTURES TO EVALUATE THEIR INFLUENCE ON OVERLAYING SEDIMENTARY LAYERS: CASE STUDY OF THREE FIELDS IN THE CENTRAL KANSAS UPLIFT

being

A Thesis Presented to the Graduate Faculty

of the Fort Hays State University, in

Partial Fulfillment of the Requirements for

the Degree of Master of Science

by

Muhammad S. Karim

B.S., Shahjalal University of Science and Technology, Bangladesh

Date_____ Approved_____
Major Professor

Approved_____
Chair, Graduate Council

GRADUATE COMMITTEE APPROVAL

The Graduate Committee of Muhammad Karim hereby approves his thesis as meeting partial fulfillment of the requirements for the Degree of Master of Science

_____
Chair, Supervisory Committee

_____
Supervisory Committee

_____
Supervisory Committee

_____
Supervisory Committee

On this day of_____

ABSTRACT

Potential field and well log data were used to investigate basement features and the overlaying sedimentary layers across four counties in the Central Kansas Uplift. The objective of this study was to (1) investigate and determine the orientation of basement structures/features, (2) estimate the depth to basement, and (3) examine the influence (if any) and relationship between the basement features and the overlaying sedimentary deposits of three oil fields in the study area. Aeromagnetic data was used to interpret and map basement features by applying derivative filters. Well log data was used to pick formation top values and create contour maps of sedimentary strata. Two major types of structural features were identified in the basement of the study location: (i) lineaments representing faults that mostly trend NE-SW and NW-SE, and (ii) basement highs that highlight two well known basement features: the Russell and Rush ribs. The estimated depths to basement using the Source Parameter Imaging (SPI) technique for aeromagnetic data vary between -112 m (-368 ft.) and -1287 m (- 4222 ft.) subsea. The inaccuracy of estimated SPI depths from the aeromagnetic data vary between -22% and 10% of the actual depths obtained from well log data. Contour maps of formation tops of the Arbuckle Group the three fields show antiforms with gentle slopes (~< 15 m/ km), channel-like, and karst features. Structures mapped in the Arbuckle appeared to be influenced by basement topography and basement lineaments (mostly faults). Contour maps of the sedimentary layers (e.g., Lansing-Kansas City Group), overlaying the Arbuckle in most of the study location show broad and flat-topped deposits with no significant structural influence from the basement. Our results show considerable structural influence of basement structures on sedimentary layers directly overlaying it.

ACKNOWLEDGMENTS

I would like to thank my advisor Dr. Hendratta Ali for allowing me to take part in this research opportunity. It sets a foundation for my future research. I would also like to thank Dr. Ali for countless hours of editing and discussing issues dealing with this project. Also, I would like to thank Dr. Chunfu Zhang and Dr. Estella Atekwana for graciously being a part of my thesis committee and providing their time and comments to ensure that this manuscript is complete and scientifically sound.

I would like to thank the Department of Geosciences at Fort Hays State University for giving me the opportunity and providing me the resources to conduct this research, the Boone Pickens school of Geology at Oklahoma State University for allowing me to work in their geophysics laboratory which was important for the advancement of specific parts of this research. I would also like to thank Dr. Neuhauser for his time and his important remarks on this project.

Finally, I would like to thank all the people who have an interest in my research and have constantly pushed me to become a better geologist, student, and most importantly a better person. I would like to thank Syed and Angeline Yaseen for their help and support throughout my school years here in Hays. Finally, I would like to thank my parents. Without them nothing was possible.

TABLE OF CONTENTS

LIST OF FIGURES

LIST OF TABLES

1. INTRODUCTION

Potential field methods (gravity and magnetics) have a long history in exploration since the 1920's (e.g., Reeves, 2005). These methods are relatively inexpensive and can cover large areas, when compared to other methods that also cover large areas such as the seismic method. For these reasons, in large scale exploration projects, potential field data are typically the first type of geophysical data that are collected and utilized. Large scale coverage using potential field methods help geophysicists to map regional scale features, to identify potential locations for detailed surveys for hydrocarbon exploration, and to identify ore bodies for mineral exploration. Potential field surveys can be conducted from land, air, marine and satellite platforms. Advancement in the acquisition and the processing of potential field data has proven to be more effective than other methods (e.g., seismic) for mapping regional basement structural trends (e.g., lineaments, faults), specific geological features (e.g., salt domes, volcanic intrusive rocks, ore bodies) and investigating environmentally inaccessible areas. For example, Peel et al., (1995) used the gravity method to study salt tectonics of Cenozoic offshore environments in the Gulf of Mexico. Pilkinton et al., (2000) employed potential field methods to identify different basement domains in a sedimentary basin in western Canada, while William and Finn (1985) used potential field methods to identify and map volcanic terranes and sub-volcanic intrusions in the Cascade Ridge of the USA. Allek and Hamoudi (2008) used aeromagnetic data to identify potential diamond exploration targets in southwestern Algeria. For hydrocarbon exploration, potential field methods have also been used to study basement structures associated with petroleum exploration in southern Tunisia (Gabtni et al., 2012) or to investigate magnetic susceptibility associated with hydrocarbon

degradation in shallow reservoirs (Ali et al., 2013). In addition, potential field methods have also been used to study neo-tectonic events; for example, Kinabo et al., (2007) used potential field methods to evaluate the early development of the Okavango Rift zone, in Botswana.

Generally, potential field methods study the contrast in specific geophysical properties within and between rock layers. Gravity methods study the density contrast in rocks, while magnetic methods study the differences in magnetic properties (e.g., magnetic susceptibility) of rocks. Generally, in the subsurface, basement rocks tend to have a higher density as well as higher magnetic susceptibility than the overlaying sedimentary rocks. For this reason, potential field data has been mostly used to study basement geology, major structures, and the tectonic framework of a region and to a lesser extent in reservoir characterization and delineation. The applications of potential field methods continue to be significant for mineral and hydrocarbon exploration.

In parts of Kansas, studies of the Precambrian basement have used various methods including some potential field methods. Some of these studies show that the basement influences the topography of the overlaying sedimentary layers (e.g., Gerhard, 2004; Newell et al., 1989; Watney et al., 2008; etc.). In other studies, using well log data, Walter (1946 and 1958) identified basement highs of the Central Kansas Uplift (CKU) that might have also influenced the overlaying sedimentary layers. The CKU is the most prominent subsurface structure in Kansas, trending NW-SE and bounded by a set of faults (Koster, 1935). These NW-SE and NE-SW trending faults were reactivated during the Phanerozoic time. Fault reactivation probably, also affected the formation of the structural and stratigraphic hydrocarbon traps of the Arbuckle and the Lansing-Kansas

City Groups. The Arbuck and the Lansing-Kansas City Grouops are two most hydrocarbon producing units in the CKU (Gerhard, 2004).

Well log data have long been used for mapping subsurface features and for hydrocarbon exploration in Kansas particularly drilled wells in the Arbuckle and Lansing-Kansas City. For example, Cole (1975) mapped sedimentary strata of Cambrian-Ordovician age to identify structural elements (e.g., folds, faults) in Kansas using well log data. However, mapping structures using well log data has several limitations that are due to: (i) variations in depth of investigation (all wells are not drilled to same depth and do not typically reach the basement rock), (ii) different spatial distribution and continuity of wells (the well spacing varies and continuity between or within fields can be lost), (iii) data availability (different well log data are collected and owned by different operators who may or may not make them available at the time of investigation), and (iv) differences in well logging dates, well logging technology, and the cost of well log data. It is therefore, beneficial to combine the high resoulution capabilities of well log data and the broad coverage of potential field data to investigate the relationship between sedimentary strata and basement rocks, especially in the CKU which is a prolific oil producing region in Kansas, and potentially host several small and yet undiscovered hydrocarbon traps.

Between 1975 and 1979, the Kansas Geological Survey (KGS) acquired state wide potential field data. After this data acquisition, several studies (e.g., Gay, 1995; Watney et al., 2008; Yarger, 1982, 1989; Xia et al., 1996; etc.) were conducted to further investigate basement geology in many parts of Kansas. For example, Gay (1995) used residual aeromagnetic data to interpret basement structures and documented how the

structural highs in petroleum bearing rocks were influenced by high and low magnetic anomalies in six fields (Moore SW, Willow Dale, Alameda, Coats, Gillian, and O.S.A. fields) found in southwestern Kansas. Watney et al., (2008), interpreted some lineaments from aeromagnetic data as basement faults to explain how these basement structures influence overlaying sedimentary layers, in six oil fields (Nicholas, Donald, Glick, Spivey-Grabs, Dickman and Victory fields) in southwestern Kansas.

Although, the statewide potential field data was used to study basement rocks in some parts of Kansas, no published study has yet examined the influence of basement features on the overlaying sedimentary layers within the CKU using the aeromagnetic data and/or combined with well log data. The purpose of this study is to use the aeromagnetic and well log data to examine the relationship between basement features and sedimentary layers across four counties in the CKU.

2. OBJECTIVES

The objectives of this study are to: (1) Investigate and determine the orientation of basement features across four (Ellis, Russell, Rush and Barton) counties in Kansas. (2) Estimate the depth, from the surface to the basement rocks in the study area. (3) Examine the influence (if any) of basement features (e.g., structures) on the overlaying sedimentary deposits.

3. LOCATION

The study area covers four counties in north central Kansas (USA). These counties include: Ellis, Russell, Rush and Barton counties. These four counties are located between latitude 39º30”- 38º00” N and longitude 98º00”- 100º00” W (Figure 1).

Three field locations (including two known oil fields and one cluster of oil fields) were selected within the study area for additional investigations using well log data. The location of the fields within the study area are shown in Figure 1. The three fields include: 1) the Bemis-Shutts field (located along the crest of the CKU), 2) the Ellis Cluster field (located in the northwestern part of the CKU), and 3) the Kraft-Prusa field (located in the southeastern part of the CKU). The Ellis Cluster field is comprised of a grouping of 10 smaller oil fields, including the Ellis field, Ellis Southeast field, Ellis Southwest field, Ellis Northwest field, Ellis West field, Ellis East field, Raynesford field, Raynesford East field, Kraus field, Pleasant field, and Irvin field. The cluster was created because these fields are very close together, share a similar geological setting, and when combined are comparable in size to the other two fields.

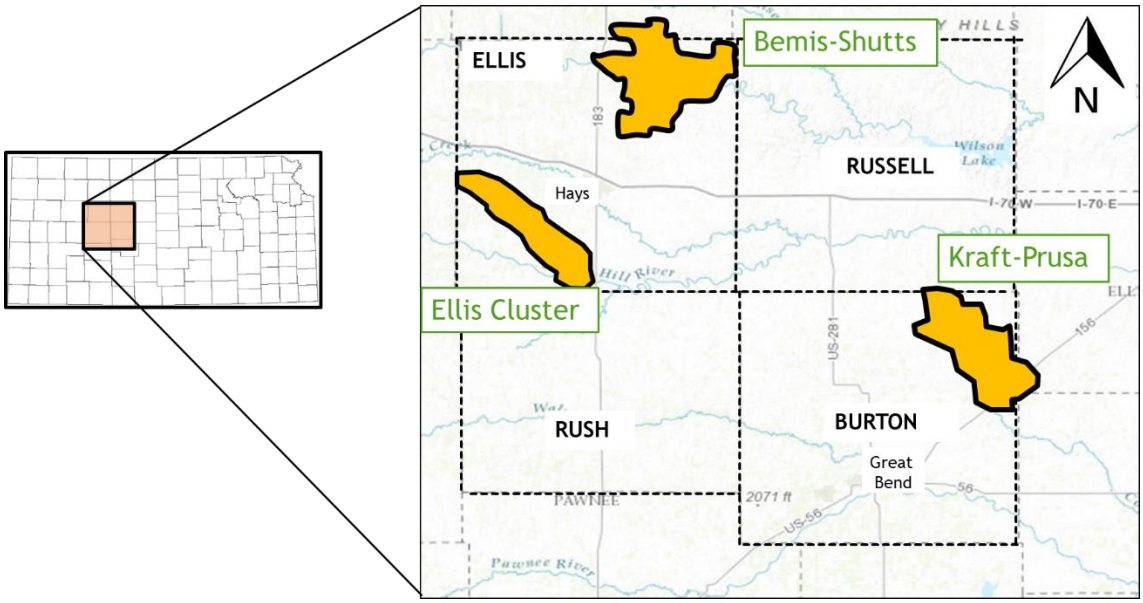

Figure 1: This figure shows the study location (four counties and selected fields). The orange square shows the location of the four counties (left). Three outlined polygons are selected oil fields (right). The Bemis-Shutts field is located to the north, the Ellis Cluster field (composed of 10 small fields) is located to the west and the Kraft-Prusa field is located to the south-east of the study location.

4. GEOLOGICAL BACKGROUND

4.1. Distribution and Nature of Precambrian Rocks

Precambrian rocks in Kansas are part of a platform-like extension of a large continental craton known as the Canadian Shield (Merriam, 1963). Figure 2 shows the distribution of Precambrian rocks in Kansas, which are divided into two rock terranes, with one terrane to the north and the other terrane to the south (Van Schumes et al., 1987) of the State.

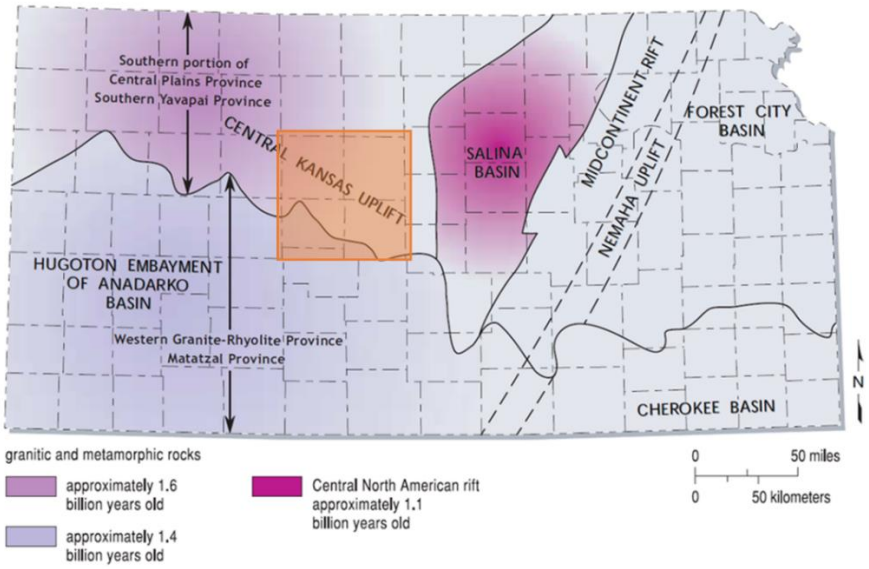

Figure 2: Generalized map of Kansas showing major basement terranes (modified from Newell et al., 1987). Ages of these terranes are color coded. Major sedimentary basins and deformational structures are also highlighted in the figure. The orange colored box shows the current study location.

The northern terrane is part of the southern extension portion of the Central Plains Province (Van Schumes et al., 1987). It is mostly composed of granitic and metamorphosed sedimentary rocks that formed ~1630 m.y. ago (Bickford et al., 1981; Yarger, 1982). The southern terrane belongs to the Western Granite-Rhyolite Province is mostly composed of younger rhyolitic rocks and epizonal granite plutons that formed ~1400 m.y. ago (Bickford et al., 1981). Xia et al., (1996) interpreted the geology of the

basement rocks in Kansas using potential field data. The study shows that most of the basement rocks in the southwestern part of the CKU are mesozonal granitic rocks (~1625 m.y. ago) with few patches of epizonal granitic rocks (~1400 m.y. ago). These different terranes of basement rocks signify a change in tectonic style from the accretion of successive volcanic arches to an extensional tectonism (Bickford et al., 1986). The change in tectonic style likely fractured the brittle basement rocks, and might have significantly influenced later structures (Gerhard, 2004) in the basement and in the overlaying rocks.

4.2. Structural Framework

The structural framework of Kansas is of great interest to exploration geologists and has been studied since oil production began in the 1920's. In 1920's, studies were mostly conducted using outcrop field mapping techniques, and subsurface investigation using the available well data. Some of these studies (e.g., Merriam, 1955) identified two major structural trends in Kansas: NE-SW trend, represented by the Nemaha Uplift and the Pratt Anticline and NW-SE trend, represented by the Cambrian Arch, the Central Kansas Uplift, and the Bourbon Arch. The CKU and the Nemaha Uplift (Figure 3) are two major basement highs which were developed during the Mississippian (Newell et al., 1987). Two sets of faults bound these basement highs. One of these fault sets is the NE-SW trending Nemaha fault zone, which bounds the Nemaha Uplift (Figure 2) and is situated in eastern Kansas. Two other sets of faults, the mid-continental rift system (MSR) and the Humboldt fault zone are also situated in the proximity of the Nemaha Uplift (Figure 3) (Baars, 1995). Despite their closeness and similar trends, these sets of

faults are separate from the fault sets bounding those bounding the Nemaha Uplift (Baars, 1995).

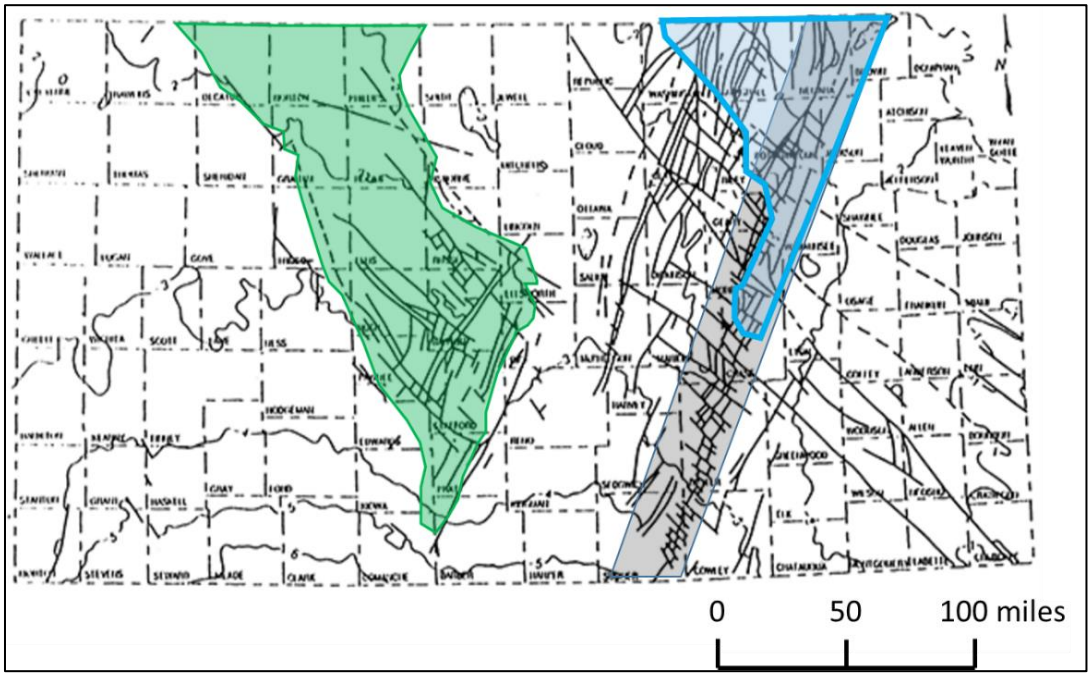

Figure 3: This figure shows the generalized fault patterns of the Precambrian basement derived from subsurface studies (Baars, 1995). The green polygon represents the NW-SE trending CKU and the blue polygon represents the NE-SW trending Nemaha uplift. The black polygon under the blue polygon represents the Humboldt fault zone.

The CKU is bounded by NW-SE trending faults and is situated in northcentral Kansas. According to Baars (1995), the southerly extension of the MRS fault zone complexly offset the southward extension of the CKU in central Kansas. The CKU where the present study site is located, was developed during the Mississippian as a result of fault reactivation in response to the stresses generated by collisional orogeny (Kluth and Coney, 1981). Before the CKU was formed, a broad NW-SE trending structural high known as the Central Kansas Arch was the major geologic feature during the Ordovician and Devonian times (Newell et al., 1987). The Central Kansas Arch was fractured by changes in tectonism during the late Proterozoic time (Gerhard, 2004). During the Mississippian, when the CKU was developing, stresses from collisional orogeny

reactivated existing fractures and faults, and created secondary uplifts (the Rush and Russell ribs) within the Central Kansas Arch (Koster, 1935).

4.3. Sedimentary Geology

Sedimentary rocks in the Central Kansas Uplift and most of Kansas typically consist of many relatively thin units that rest parallel to one another (Merriam, 1963) in a cyclical pattern. Jewett and Merriam (1959) observed that the thickness of the sedimentary deposits in Kansas vary between 170 m (560 ft.) to 3300 m (10800 ft.). Most of these sedimentary layers were deposited on a shallow-shelf marine environment. During most of the Phanerozoic, Kansas was located closer to the equator and covered in a shallow warm sea (Franseen et al., 2004; Watney, 1980; and Watney et al., 2008). Because of their environment of deposition, the sedimentary layers in Kansas are mostly composed of carbonate lithofacies (Merriam, 1963).

Throughout the Phanerozoic, tectonic events reactivated Precambrian basement faults which created some major deformational features including the Salina basin, the Forest City basin, the Central Kansas Uplift, and the Nemaha Uplifts that cover most of the State. In central Kansas, several secondary structures (e.g., Fairport anticline in Russell County, and the Rush rib in Rush County etc.) were also developed along with these major structures (Jewett, 1951). Over time, sedimentary layers in Kansas have been interrupted by seven major unconformities (Merriam, 1963) that significantly altered the stratigraphic sequence. Three of these major unconformities ware identified in the study area and are marked by erosional surfaces: 1) the erosion between late Precambrian and early Cambrian that marks the nonconformity between the Arbuckle and the Precambrian basement rocks, 2) the erosion between late Devonian and early Mississippian that marks

the disconformity between the Simpson and the Arbuckle Group) and 3) the erosion between late Mississippian and early Pennsylvanian that marks the disconformity between the Lansing-Kansas City Group and the Simpson Group (Merriam, 1963).

The reactivation of basement faults, the variations in the thicknesses of deposits and the major unconformities, have together created geometries that formed significant structural, stratigraphic, and a combination of structural and stratigraphic traps in the CKU (Gerhard, 2004). Detailed investigations of the subsurface geologic features are necessary to study these traps especially their structural elements. Figure 4 summarizes the stratigraphic relationship between rock layers in the study area. Among these deposits, the Arbuckle Group, the Simpson Group and the Lansing-Kansas City Group are the major hydrocarbon bearing units and the Heebner Shale is a major marker bed.

4.3.1. The Arbuckle Group

Rocks of the Arbuckle Group are present in most of Kansas and occur at depths between 150 m (500 ft.) and 1500 m (5000 ft.) (Newell et al, 1987). The Arbuckle strata was deposited in tidal to subtidal shallow marine environments (Wilson et al., 1991). Rocks of the Arbuckle Group are composed mostly of light grey to white cherty, vuggy dolomites (Franseen, 1994). The Arbuckle is bounded at its base and its top by two major unconformities (Sloss, 1963). The unconformity at the base is a nonconformity on the Precambrian surface (between the Arbuckle and the Precambrian basement) and the unconformity at the top is a disconformity formed during the late Devonian and early Mississippian (between the Simpson and the Arbuckle Group rocks). In Kansas, Arbuckle rocks mostly overlay the Precambrian basement, unless the Reagan Sandstone is present. The Reagan Sandstone is a basal Paleozoic transgressive sandstone unit that

typically lies directly on the Precambrian basement rocks and below the Arbuckle layer when it is present. The composition and texture of the Reagan Sandstone is markedly influenced by the underlying basement rock. The Reagan can either be quartzose, arkosic, or feldspathic; texturally it can range from fine to coarse grained (Newell et al., 1987). The Arbuckle Group can be as thick as 160 m (550 ft.) in the central Kansas (Walter, 1958), whereas the thickness of Reagan sandstone averages 13 m (40 ft.) or less wherever it is present in Kansas (Newell et al., 1987).

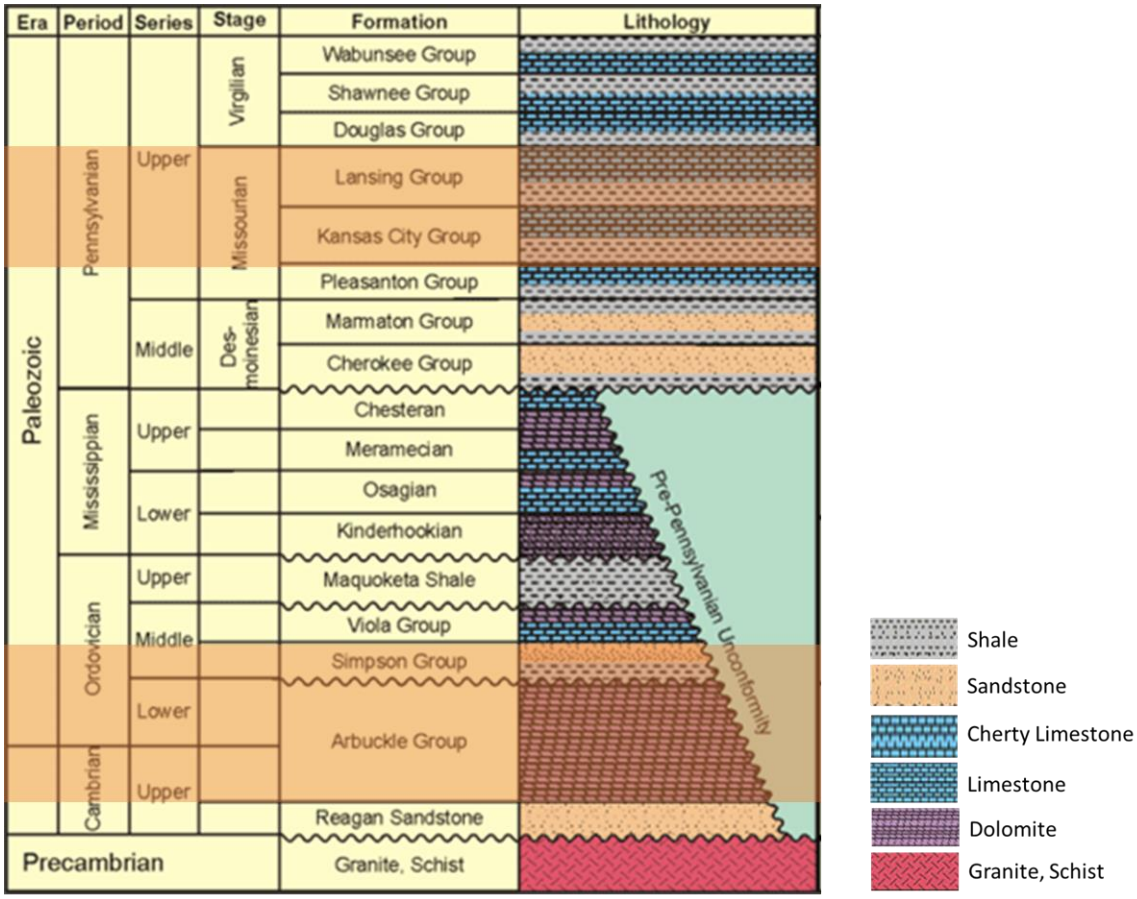

Figure 4: Generalized stratigraphic column of the Central Kansas Uplift. Highlighted sections show the intervals present in the study location (after Cansler and Carr, 2002).

Cansler and Carr (2002) report that the Arbuckle Group was affected by the rejuvenation of basement structures that resulted in fractures, regional uplifts, and minor

horst and graben features. In addition, the Arbuckle was modified by karst processes during periods of prolonged and repeated subaerial exposure that began after the Arbuckle deposition, and continued in some areas until the Pennsylvanian period (Franseen, et al., 2004). The combination of these deformational and depositional processes led to the formation of structural, stratigraphic, and combination of structural and stratigraphic hydrocarbon traps, making rocks of the Arbuckle Group the most significant oil producing strata in the CKU (Newell et al., 1987).

4.3.2. The Simpson Group

The Simpson Group rocks are primarily present in the south-central part of Kansas, although thinner layers are present in a few places within the CKU (Newell et al., 1987). The Simpson Group is the basal unit of rocks which were formed during the long term oceanic inundation on the North American continent and is dominantly composed of a sand-shale sequence with minor amounts of carbonate rocks (Adler, 1971). Late Mississippian to early-Pennsylvanian tectonism removed the Simpson Group over much of the CKU (Merriam, 1963). In addition, the sub-Pennsylvanian erosion truncated the Simpson Group along the periphery of the CKU (Newell et al., 1987). Fault reactivation, erosional truncation and lithological characteristics of the formation (interbedded shale and sandstone sequence), together formed potentially significant hydrocarbon traps in the Simpson Group wherever it is present in the CKU (Newell et al., 1987).

4.3.3. The Lansing-Kansas City Group (LKC)

Rocks of the Lansing-Kansas City Group are present in most of Kansas. The rocks that makeup the group are thicker in the basin areas of the state (e.g., Salina basin) compared to the thicknesses typically observed on the CKU (Watney, 1980). On the CKU, the Lansing-Kansas City Group directly overlies the Arbuckle Group in areas

where Mississippian and Ordovician deposits (e.g., the Simpson Group, Viola Group, etc.) were eroded by sub-Pennsylvanian erosion (Merriam, 1963).

The LKC Group is composed of interbedded carbonates and shales with occasional minor coal beds, siltstones, and sandstones (Watney, 1980). In northwestern Kansas, the interbedded limestones and shales of the LKC are components of a cyclothem. Each cycle of the cyclothem is characterized by four components: a thin but distinctive basal transgressive unit (deposited as sea level rose), overlain by a marine shale, followed by the regressive carbonate, and a regressive shale unit (Watney, 1980). The Lansing-Kansas City Group was deposited over an extensive area of a broad shelf margin and its sedimentary structures were influenced by contemporaneous local shelf topography and multiple episodes of erosion caused by basement uplift (Baars and Watney, 1989). For these reasons, structural, stratigraphic, and combination of structural and stratigraphic hydrocarbon traps were formed by the rocks of the Lansing-Kansas City Group (Rascoe and Adler, 1983).

4.3.4. The Heebner Formation

The Heebner Formation is one of seven formations comprising the Shawnee Group (Merriam, 1963). The Heebner is an important formation because it is a marker bed that is used as a datum for much of the stratigraphic and structural work in the subsurface of central and western Kansas (Jewett and Merriam, 1959). The Heebner Formation is composed of black shales and has very high gamma ray readings which makes it easier to identify from well logs (e.g., Gamma ray).

5. METHOD AND DATA

5.1. Principles of Magnetic Survey

Magnetic surveys are designed to study small perturbations in Earth's magnetic field. These perturbations are due to the anomalous magnetic signatures from different subsurface rocks. The presence of magnetic materials in subsurface rocks generate a magnetic field known as the anomalous magnetic field. The anomalous magnetic field of any subsurface rock is induced by the stronger magnetic field produced from Earth's core. This larger and stronger field is known as Earth's main magnetic field or the geomagnetic field. The magnetic intensity of the geomagnetic field varies from 20,000 nT to 70,000 nT (Reeves, 2005). Typically, during a magnetic survey the total magnetic field intensity data (the main magnetic field and the anomalous magnetic field together) are acquired.

The anomalous magnetic field of subsurface rocks depend on the magnetic susceptibility of the materials in the rock. The magnetic susceptibility of a material indicates the degree or extent to which the substance can be magnetized in response to an applied magnetic field (Robinson, 1988). This magnetic susceptibility of a material relies on the combined effect of electron motions and spin orbitals in atoms to produce strong magnetism within small regions of a substance known as magnetic domains (Robinson, 1988). Based on their susceptibility, magnetic materials can be grouped into four types: diamagnetic, paramagnetic, ferromagnetic, and anti-ferromagnetic material (Reeves, 2005). The response of diamagnetic and paramagnetic materials in a magnetic field is very negligible, and these materials are generally described as non-magnetic materials. Thus, they are not significant for magnetic survey responses. Ferromagnetic materials get

magnetized relatively easily when placed in a magnetic field along the field lines (Robinson, 1988). Only a few groups of material (typically those containing iron, nickel, cobalt or some of their alloys) have strong magnetic domains and are ferromagnetic. In the case of anti-ferromagnetic materials, magnetic domains cancel each other out to give zero magnetization. Generally, most magnetic materials of geological significance are imperfectly anti-ferromagnetic (Reeves, 2005). Magnetic surveys aim to record the response of ferromagnetic materials in the subsurface.

Aeromagnetic survey is the most common technique for acquiring magnetic data. The technique is designed to acquire subsurface magnetic data using an airborne magnetometer mounted on an aircraft. For convenience of data collection, the aeromagnetic technique only measures the scalar magnitude of the total magnetic field intensity (Reeves, 2005), although the magnetic field of the Earth or any other magnetic body occurs as a vector quantity that requires three scalar components.

After collecting the total magnetic intensity data, the geomagnetic field component is removed by using the International Geomagnetic Reference Field (IGRF), to get the local magnetic anomaly. Different temporal variations (e.g., diurnal variations, micro-pulsations, magnetic storms, secular variation etc.) have profound impacts on the local IGRF reading. Therefore, the effects of all these variations are also removed from the total magnetic field intensity before any interpretations are made. Due to the complex nature of magnetic properties, the solutions derived using magnetic methods are non-unique. For this reason, different spectral filtering techniques have been developed to enhance the geological interpretation of data obtained from magnetic surveys.

5.2. Spectral filters

Spectral filters are mathematical algorithms which are applied to magnetic data in a spectral domain or a wave domain, and involve vector quantities in three directions. Usually, aeromagnetic data is collected only in the spatial domain and then transformed to the spectral domain before filters are applied using Fast Forward Fourier transformation (Yarger, 1982). Once the filter is applied, the data is transformed back into the spatial domain and then displayed on a map, a profile or a 3D model (Gunn, 1975). The purpose of spectral filtering is to remove unwanted characteristics depending on the interpretation objectives and enhance the quality of the data. The following spectral filters were applied to the aeromagnetic data used in this study.

5.2.1. Reduction to Pole

Reduction to pole (RTP), is a filter that removes the effect of the inclination and declination of the geomagnetic field. RTP removes the skewness of the anomalies and directly positions magnetic anomalies over their sources. RTP assumes a uniform direction of magnetization (geographic north-south) for all anomalous magnetic source bodies which are magnetized by the geomagnetic field (MacLoed et al., 1993). The effect of magnetization of the geomagnetic field on any magnetic source body depends on the orientation of the geomagnetic field direction at that location. The orientation of the geomagnetic field (imaginary lines from one magnetic pole to the other) vary at different geographic locations because of the Earth's rotation and the dipole nature of geomagnetic field (Reeves, 2005).

The magnetic inclination and declination at any given location on Earth, indicates how the orientation of the geomagnetic field varies at that location from the geographic

north-south direction. The angle between the geomagnetic north (the direction the north end of a compass needle points) and geographic north of the Earth is known as declination. On the other hand, magnetic inclination is the angle between the geomagnetic field direction and a horizontal plane (Robinson, 1988). According to Grant and Dodds (1972), the RTP operator can be expressed as,

$$L(\theta)=\frac{1}{[\sin(I)+i\cos(I)\cos(D-\theta)]^2}$$

Where, θ is the magnetic field direction, D is declination and I is inclination. When the data used in this study was collected between 1975 and 1979, the average declination and inclination values in Kansas was D=67.8˚and I=6.78˚.

5.2.2. Vertical Derivative

The vertical derivative filter (VDR) is a mathematical expression to determine how the magnetic anomaly changes with respect to depth from the surface. The vertical derivative filter narrows the width of anomalous bodies and makes it easier to locate and delineate source bodies that have anomalous magnetic fields (Cooper and Cowan, 2004). Generally, higher order (e.g., 2nd order) vertical derivatives show better results for delineating source body structures. However, higher order vertical derivatives are also much more sensitive to the noise in the data, which can be difficult to eliminate. For this reason, it is sometime preferable to apply the 1st order vertical derivative to a data set to minimize the effect of noise. The VDR was also selected because of its ability to delineate linear features. As presented earlier, previous studies have shown that most of the basement structures across the CKU are contacts (e.g., faults) with fewer structural highs (e.g., the Russell rib). The basic mathematical expression for the 1st order vertical derivative (Miller and Singh, 1994) is given by,

$$\text{VDR} = \frac{dT}{dz}$$

Where, VDR= 1st order vertical derivative, T = the total magnetic field intensity and z = depth.

For the data set in this study, the 1st order VDR was used. This was selected because the data was acquired relatively long ago between 1975 and 1979 and susceptible to having more noise than recently acquired data.

5.2.3. Tilt Angle Derivative

The tilt angle derivative (TDR) is a mathematical expression to determine the rate at which the tilt angle changes with respect to the depth of the magnetic anomalies, from the surface. The tilt angle is given by the inverse tangent of the vertical derivative over the total horizontal derivative of any magnetic source body. The tilt angle estimates the magnitude of the rate of change of the total magnetic intensity in all directions and normalizes all the edges in the data. In general, for 1st order vertical derivative, the values over magnetic source bodies are positive, over the edge of the source bodies the values are zero and at the base of the magnetic source bodies the values are negative (Miller and Singh, 1994). For the horizontal derivative, the values at the edge of the magnetic source bodies are positive, and the values at the top of the magnetic source bodies are zero (Miller and Singh, 1994). Given that the tilt angle derivative is the ratio of vertical and horizontal derivatives, it does not require any prior approximation of the magnetic source body structure. The anomaly on a tilt angle derivative map is maximum at the top of a magnetic source body and minimum at the base of the source body (Salem et al., 2007). Therefore, positive tilts from TDR maps show the top of source body structures, whereas negative tilts show the base of source body structures. A map of tilt derivative shows the

tilting of source bodies, with maximum tilt at 90° and minimum tilt at -90° (Verduzco et al., 2004). The tilt angel derivative is given by the relation,

$$\text{TDR}=\frac{d\theta}{dz}$$

Where, TDR = tilt angle derivative, and θ = tilt angle and *z* is depth. $\theta = \tan^{-1}\frac{\left(\frac{dT}{dz}\right)}{\left(\frac{dT}{dh}\right)}$ and $\left(\frac{dT}{dh}\right) = \sqrt{\frac{dT}{dx}+\frac{dT}{dy}}$. $(\frac{dT}{dx}), (\frac{dT}{dy}), and\ (\frac{dT}{dz})$ are derivatives of three components of magnetic field intensity and $\left(\frac{dT}{dh}\right)$ is the total horizontal derivative. In general,

$$\text{Tilt Derivative (TDR)} \;=\; \tan^{-1}\left(\frac{\text{VDR}}{\text{HDR}}\right) \text{ in Radians}$$

The Tilt derivative range is restricted to $-\frac{\pi}{2} \leq \text{TDR} \leq +\frac{\pi}{2}$ or (-90° ≤ TDR ≤ +90°).

5. 3. Depth Estimation from Magnetic Data using Source Parameter Imaging (SPI)

Source parameter imagining (SPI) is a depth estimating technique used to determine the depth to basement from the ground surface using the local wavenumber of the analytical signal (Roest et al., 1992, and Smith et al., 1998).

The analytical signal is given by,

$$A\,(x,z) = \frac{dT(x,z)}{dx} - j\,\frac{dT(x,z)}{dz}$$

Where, *A (x, z)* is the analytical signal, *T(x,z)* is the magnitude of the anomalous total magnetic field, *j* is an imaginary number and x and z are Cartesian coordinates of the vertical and horizontal directions perpendicular to the strike of the magnetic source bodies.

The local wavenumber of the analytical signal is defined by Thurston and Smith (1997) to be:

$$\text{K}_1 = \frac{d}{dx}\,\tan^{-1}\left(\frac{dT}{dz} \Big/ \frac{dT}{dx}\right)$$

Where, K_1 is the local wavenumber and $(\frac{dT}{dz})$ and $(\frac{dT}{dx})$ are derivatives of total magnetic field intensity in the *z* and *x* direction.

The analytical signal (A) value is highest over the edge of the magnetic source bodies (Nabighian, 1972); therefore, the edge of any magnetic source body is represented by the maxima of the local wavenumber of the analytical signal. These maximum values of the local wavenumber are the edges of anomalies that can be used to define the location of the anomalous source body. The result of the analytical signal is independent of the inclination of the Earth's field and the amplitude of the analytic signal simply relates to the magnetization of the source body. The result is largely immune to anomaly distortion due to permanently magnetized sources. An advantage of this SPI method is that it can display depth as an "image" assuming either contacts (e.g., faults) or dipping thin sheets (e.g., dike) models (Smith et al., 1998).

5.4. Aeromagnetic Data

The aeromagnetic data used in this study were acquired by the KGS between 1975 and 1979 (Xia et al., 2000) as previously discussed. All airborne magnetic data are usually acquired along flight-lines that represent the path of the aircraft carrying the magnetometer used for data collection. Spacing between flight-lines is important for data resolution. Generally, the closer the spacing of flight-lines, the better the resolution of the data acquired. For the data set used in this study, flight-lines were flown from east to west and spaced 3.2 km (2 miles) apart. On average 90 to125 readings were gathered every meter along each flight-line (Xia et al., 2000). A smaller amount of data was also collected in the direction normal to the flight-lines (north to south), to provide some additional controls on the temporal variation of the geomagnetic field. These perpendicular lines to the flight-lines are known as tie-lines. The spacing between tie-lines are usually about ten time the spacing of flight-lines. For the data set in this study,

tie-lines were flown in the north-south direction and were spaced 32 km (20 miles) apart. Figure 5 shows a layout of the general direction of flight-lines and tie-lines for this data set.

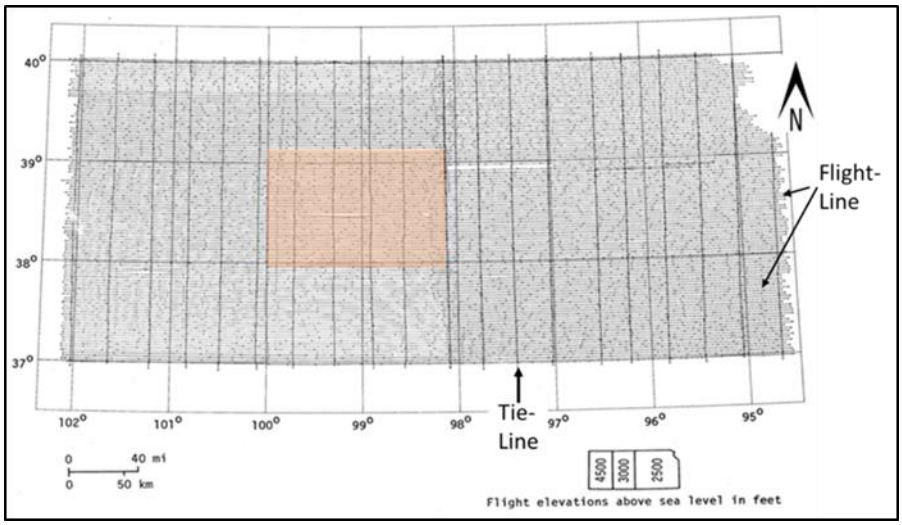

Figure 5: Magnetic survey grid map over Kansas showing the survey flight-lines and tie-lines. The highlighted box shows the study location

Flight-height is another crucial factor for data resolution. The lower the flight height of the airborne magnetometer from the anomalous magnetic source bodies, the better the resolution of the features. However, lower flight heights limit the depth of investigation. Usually, most anomalous source bodies are found in the basement rocks of any survey area. The flight height is therefore determined based on the thickness of the sedimentary layers of the area. In Kansas (including the location of this study), the thickness of the sedimentary strata varies between ~170 m (560 ft.) and ~3300 m (10800 ft.) (Jewett and Merriam, 1959). For this reason, the statewide aeromagnetic survey was acquired using flight heights that varied between 915 m (3000 ft.) in the eastern part and 1372 m (4500 ft.) in western part of the State where the basement is deeper. The flight heights for both the flight-lines and tie-lines were measured relative to mean sea level.

The flight heights above the CKU where our study area is located averages 914 m (3000 ft.) above mean sea level.

5.5. Well Log Data

The well log data used in this study was mainly Gamma ray (GR) and mud log data obtained for wells drilled in the three field locations (the Bemis-Shutts field, Ellis Cluster field, and Kraft-Prusa field) as described earlier. The well log and mud log data were used to pick formation top values that were contoured to create maps. Most of these wells were drilled by local oil and gas companies. The well data was collected and stored by the Kansas Geological Survey and made available through their website (www.kgs.ku.edu). The formation tops contour maps were created using the mapping software (IHS Petra©) by applying the Kriging algorithm. The number of wells that were used to generate contour maps for each of the field locations are: 2271 wells from the Bemis-Shutts field, 910 wells from the Ellis Cluster field, and 1575 wells from the Kraft-Prusa field. Contour maps were generated for formation tops of four formations including the Arbuckle Group, the Simpson Group (only in the Bemis-Shutts field), the Lansing-Kansas City Group and the Heebner Formation.

6. ANALYSIS AND INTERPRETATION

6.1. Magnetic Derivative Maps of the Basement

6.1.1. Total Magnetic Intensity Map

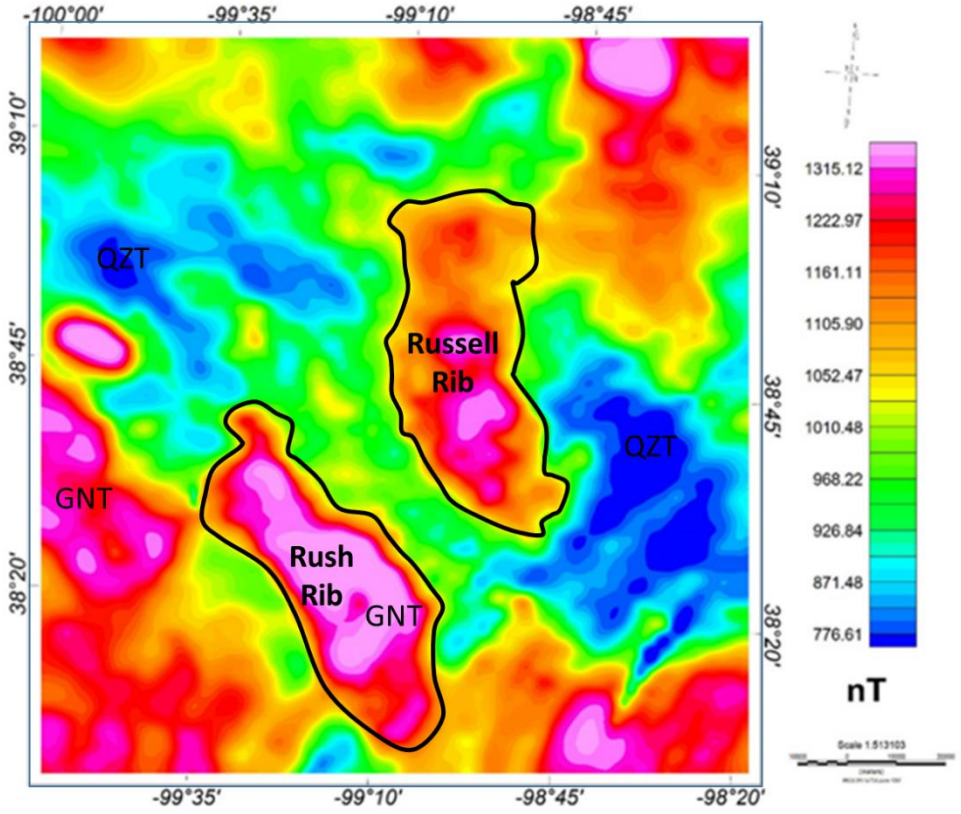

Figure 6: The total magnetic intensity (TMI) map (after applying reduction to pole (RTP) spectral filter) of the study area. The two relatively high magnetic anomalies (in the middle and in the southeastern part of the study area) correspond to the structurally high Russell and Rush ribs. GRT represents areas with granitic rocks and QZT represent areas with quartzite rocks.

The total magnetic intensity (TMI) map (Figure 6) shows the distribution of the magnetic anomaly across the study area. The TMI map is generated after applying the reduction to pole (RTP) spectral filter using magnetic inclination and declination values at the study location, when the data was acquired. The basement rocks in the study area are granite-rhyolite to metasedimentary rocks, and show magnetic intensity values between 770 nT and 1315 nT. On the TMI map the warm (bright) colors (yellow to pink)

with magnetic intensity values greater than 1050 nT, represent the granitic basement rocks (that typically have higher magnetic content compared to quartzites) (Hankel et al., 2002). The two zones in the middle of the study location outlined showing high magnetic anomalies are identified as the Russell and Rush ribs. The cold (dark) colors (greens to blues) with magnetic intensity values less than 900 nT, represent basement rocks that have a lower content in magnetic materials. In the study area, the dark blue colors with magnetic intensity values less than 700 nT in the south-east portion represent the quartzite rocks.

6.1.2. Vertical Derivative Map

The vertical derivative (VDR) map of the study area (Figure 7) is generated from the TMI grid after applying the RTP filter. The VDR magnetic anomalies in the study area vary between 0.05 nT/m and -0.05 nT/m. Based on previous studies (e.g., Baars, 1995; Newell et al., 1989; Watney et al., 2008; etc.), which show that most of the basement features in the study location are linear structures (mostly faults), linear magnetic anomalies with low values (< -0.018 nT/m) are interpreted as faults and highlighted with black and white solid lines on Figure 7.

Interpreted basement lineaments mostly trend NW-SE and NE-SW. On the VDR map, the NW-SE trending lineaments (white solid lines) appear to be truncated by the NE-SW trending lineaments (solid black lines) in the southeastern corner. This observation is consistent with various previous studies (Baars, 1995; and Van Schumes and Hinze, 1985) that show NE-SW trending lineaments (extensions of MRS fault zone) truncating NW-SE trending lineaments on the southeastern part of the CKU. Baars (1995) interpreted the intersection of these two major fault zones as conjugate sets in

central Kansas. These conjugate sets of faults were reactivated during the Mississippian when the CKU was developed. Therefore, sedimentary layers (mostly pre-Mississippian strata) directly overlaying the Precambrian basement should show the influence of both the NE-SW and NW-SE basement structural trend within the CKU.

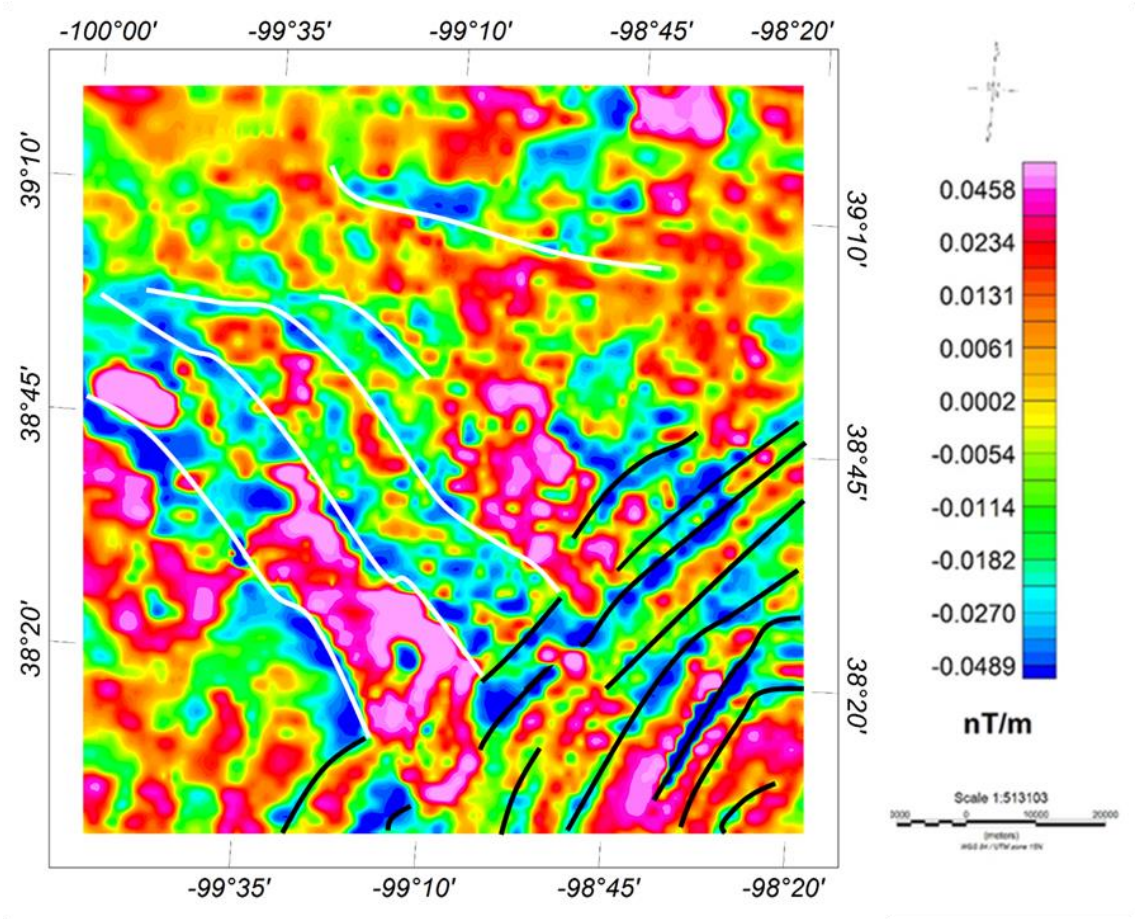

Figure 7: The vertical derivative (VDR) map of the study area. The black solid lines represent NE-SW trending lineaments and the white solid lines represent NW-SE trending lineaments.

6.1.3. Tilt Angle Derivative Map

The tilt angle derivative (TDR) map (Figure 8) is generated from the same TMI grid after applying the reduction to pole filter. On the TDR map the values of tilt angle derivative vary between 1.2 rad/m and -1.3 rad/m.

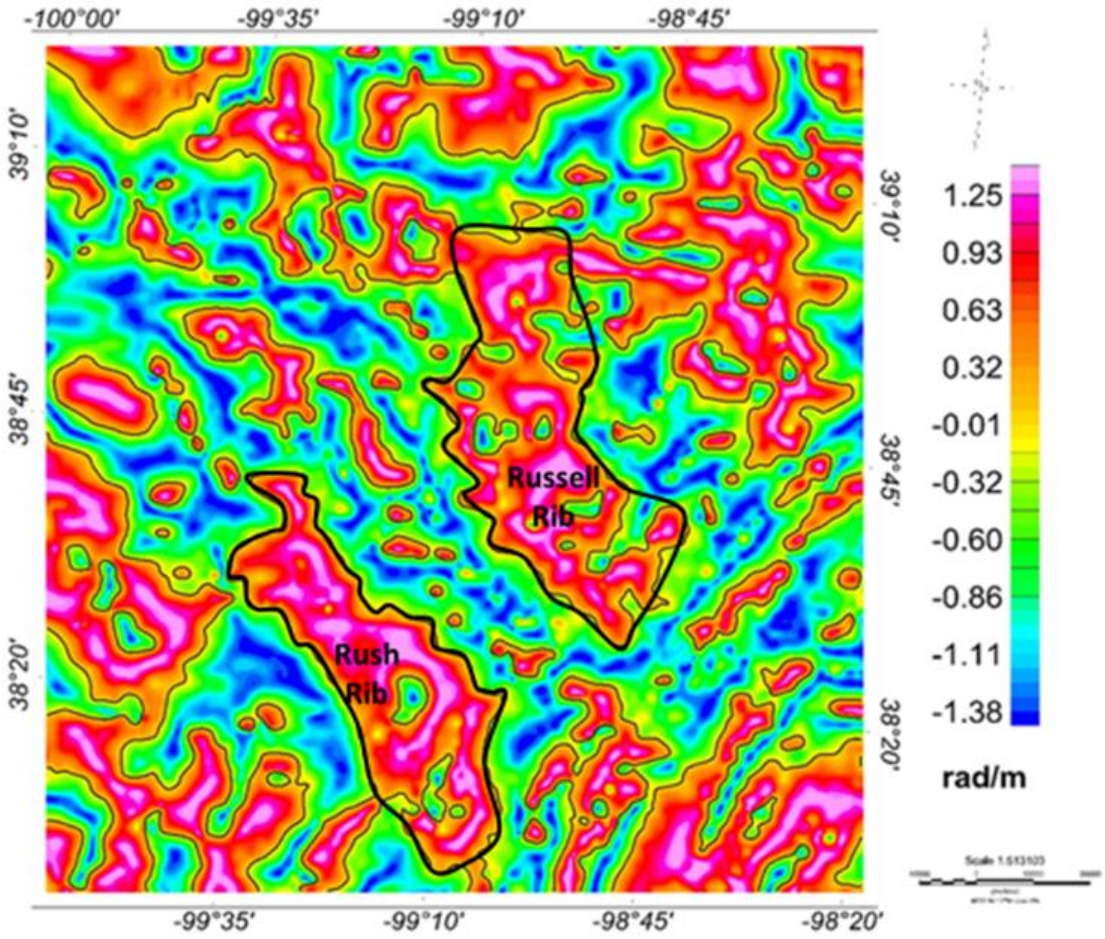

Figure 8: The tilt angle derivative (TDR) map of the study area. The thin black lines are zero contour lines representing the edge of the magnetic source bodies. The NW-SE trending Russell and Rush ribs are outlined with thicker black lines.

The warm colors represent positive tilt (TDR greater than 0.8 rad/m), which indicate the top of magnetic source bodies (e.g., epizonal granitic pluton) whereas, the cold colors represent negative tilt (TDR less than -0.9 rad/m), which indicate the base of magnetic source bodies or basement faults. The zero-contour lines (thin black color) are drawn on the TDR map to represent the edge of anomalous source bodies. The Rush rib and the Russell rib previously interpreted, are outlined with thicker black zero-contour lines in the southwest section and in the middle portion of the map. Both the Rush and

Russell ribs, trending NW-SE, are observed to be crosscut by NE-SW trending basement lineaments on the southeastern part of the study area.

6.2. Depth Estimation

6.1.3. Source Parameter Imaging Map

The source parameter imaging (SPI) map (Figure 9) is generated from the same TMI grid as the previous maps.

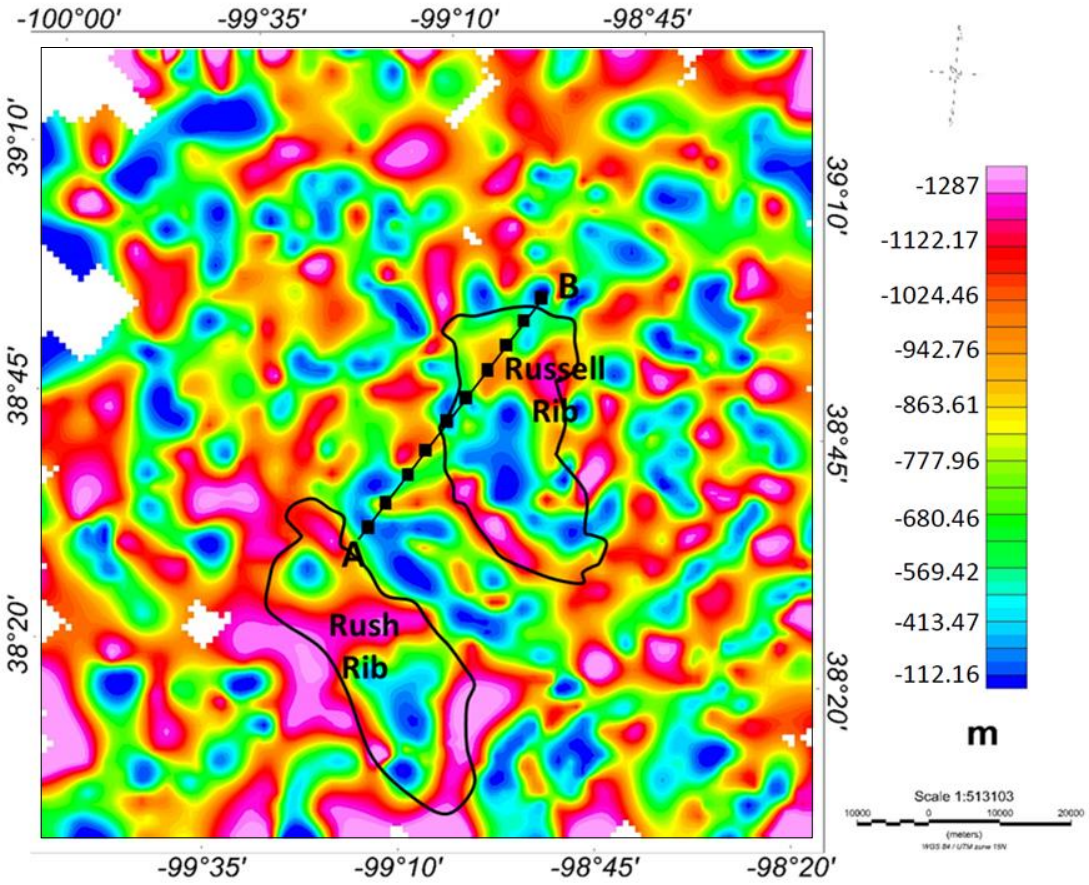

Figure 9: The source parameter imaging (SPI) map of the study area. The deeper parts <-1290 m (-4232 ft.) subsea of the basement are shown in warm colors and the shallower parts >-112 m (-368 ft.) subsea of the basement are shown in cold colors. The outlined areas show the two known structurally high Russell and Rush ribs. *Note:* The gaps on the map are areas where the estimated depth from the SPI exceeded the set depth limit of -1900 m (-6234 ft.) for the study area. Depth limit was set to -1900 m (-6234 ft.) because no well from the study area had a basement surface deeper than -1900 m (-6234 ft.) subsea.

Twelve depth values from both SPI and basement tops contour map are selected along the line A-B to check the accuracy of the estimated depths from the SPI method. Assuming that most of the basement structures are faults, the SPI method is applied to gridded data for dipping contact (fault) model. The estimated SPI depths vary between -112 m (-368 ft.) and -1287 m (-4220 ft.). The estimated depths to basement on the SPI map (Figure 9) are subsea depths. The values that are less than -1025 m (-3362 ft.) represent the deep basement surface, whereas the values greater than -413 m (-1355 ft.) represent the shallow basement surface. The locations corresponding to the Rush and Russel ribs, have shallower basement surface and are highlighted in blue.

6.2.2. Basement Tops Contour Map

The contour map from wells that penetrated the Precambrian basement does not cover the entire study area because of the limited number of wells that are drilled to the basement. However, the well data obtained and contoured, provides a good estimation of depth to the basement surface across the key portion of the study area. The estimated depths from the basement tops contour map are subsea depths (Figure 10) and vary between -637 m (2090 ft.) and -451 m (1480 ft.). The depth values higher than -600 m (1968 ft.) represent the deeper basement surface and the depth values lower than -450 m (1476 ft.) represent the shallower basement surface.

6.2.3. Depth Comparison from SPI and Basement Tops Map

The estimated depths from the SPI and the contour map of basement tops from well data (Table 1) are compared for data points along the profile from A to B shown on Figures 9 and 10. The comparison show that depths estimated from the SPI map are 22% lower to 10% higher than the actual depths determined from basement tops contour map.

The deviation of SPI depth values from the actual depths obtained from well log data (top to the basement) was determined as follows:

Accuracy of SPI depth compared to the actual depth=

$$\frac{Depth\ from\ the\ SPI - depth\ from\ the\ basement\ tops\ contour\ map}{depth\ from\ the\ basement\ tops\ contour\ map} \times 100\%$$

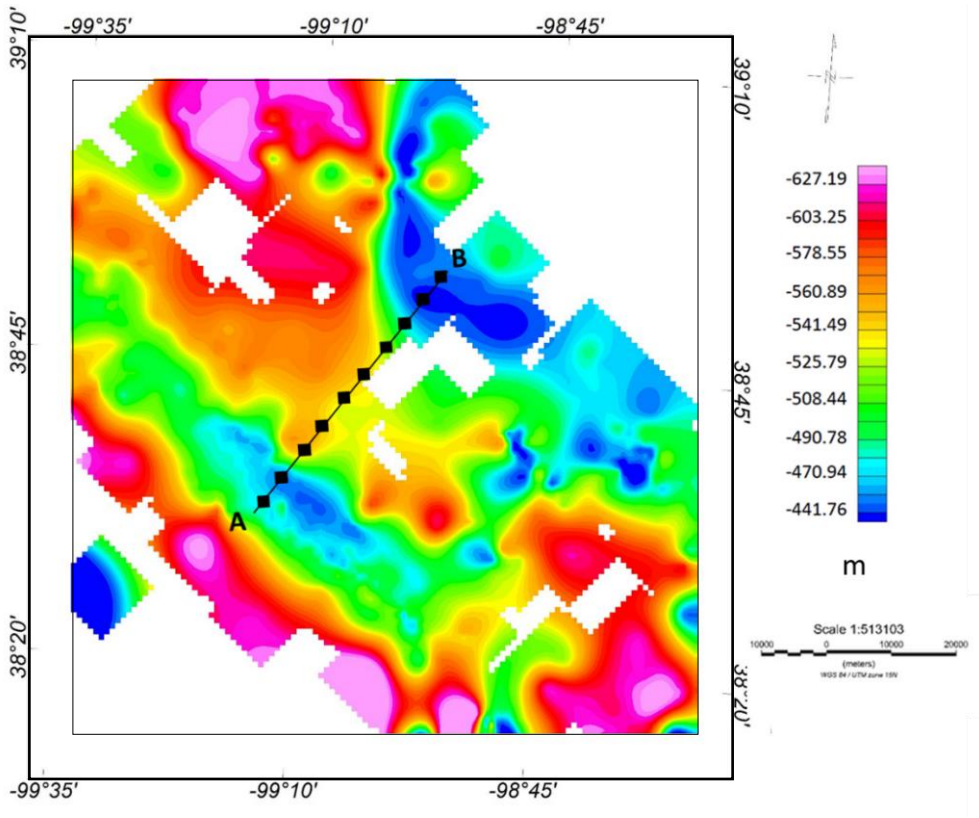

Figure 10: The contour map of basement tops. The deeper parts <-627 m (-2057 ft.) subsea of the basement are shown in warm colors and shallower parts >-441 m (-1445 ft.) subsea are shown in cold colors. Note: The gaps on the map are areas where depth values from the well log were not available.

Studies have shown that the estimated depths from the SPI method have ±20% inaccuracy compared to the actual depths to basement (Smith and Salem, 2005). The SPI results from this study are close to the range described by Smith and Salem (2005). One reason for the differences between depths obtained from the SPI and the depths from well data might be because the depths from the SPI method depend on the locations of the

anomalous magnetic source bodies (which are not always located on the basement surface). Formation tops are usually the actual depths of two layers, representing the surface of the formation, in this case the basement. Thus, in the absence of well control, SPI can be an effective way to estimate the maximum possible thickness of a sedimentary layer. Another advantage of SPI is that it is a magnetic survey method that can cover larger areas.

	Longitude	Latitude	SPI depth (m)	well log depth (m)	Difference
A	-98.84	38.79	-539.62	-443.34	-22%
	-99.13	38.58	-581.65	-478.05	-22%
	-98.86	38.78	-551.58	-458.69	-20%
	-98.79	38.83	-525.96	-441.33	-19%
	-99.26	38.48	-657.60	-573.21	-15%
	-98.94	38.72	-554.48	-505.37	-10%
	-98.85	38.79	-448.13	-451.00	1%
	-99.18	38.54	-463.27	-469.95	1%
	-99.19	38.53	-454.23	-483.55	6%
	-99.25	38.49	-517.90	-556.36	7%
	-99.14	38.58	-426.45	-466.05	8%
B	-98.95	38.71	-458.16	-509.08	10%

Table 1 Estimated depths to basement from SPI and contour map of basement tops. The locations of sample points are shown in Figure 9 and 10 along the profile A to B.

6.3. Deformation Structures in Sedimentary Layers

Figure 11 shows an overlay of selected field locations on the TMI map of the study area.

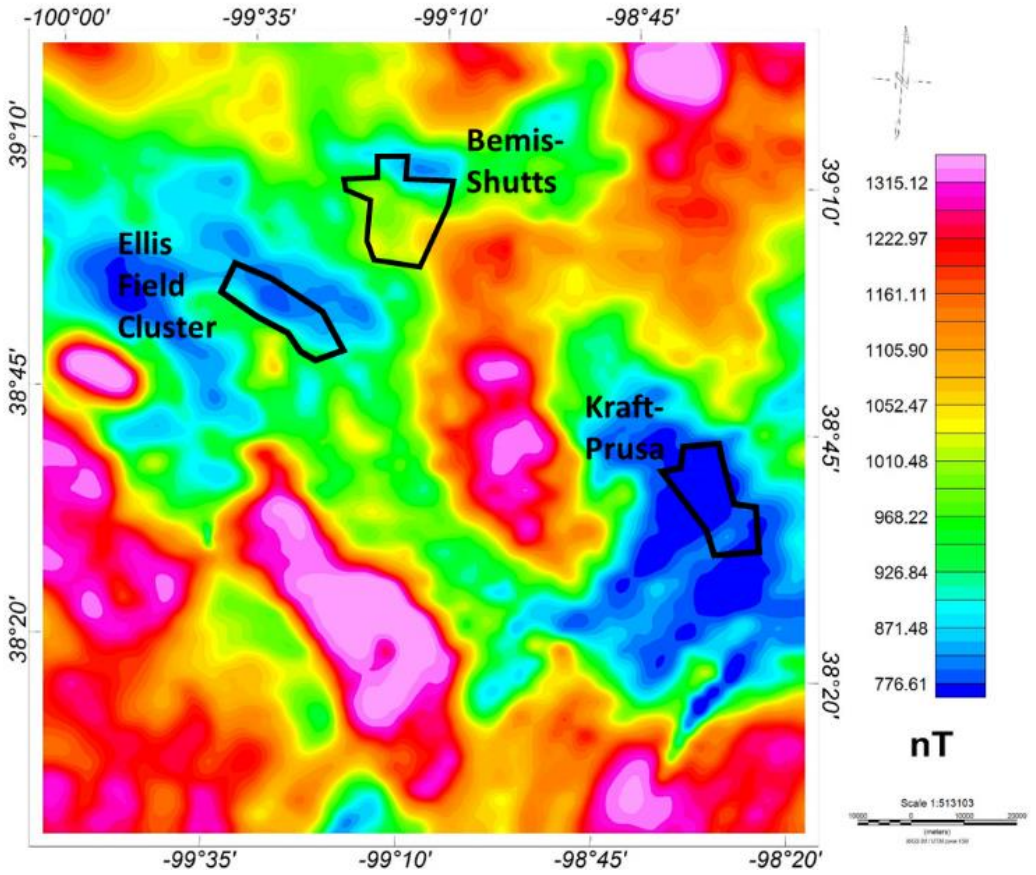

Figure 11: The total magnetic intensity (TMI) map of the study location showing outlines of selected fields (Bemis-Shutts field, Ellis Cluster field and Kraft-Prusa field).

Contour maps are generated for formation tops of the Arbuckle Group, the Simpson Group (only for the Bemis-Shutts field), the Lansing-Kansas City Group and Heebner Formation at these fields. The stratigraphic relationships between the formations of the study area are shown on Figure 12.

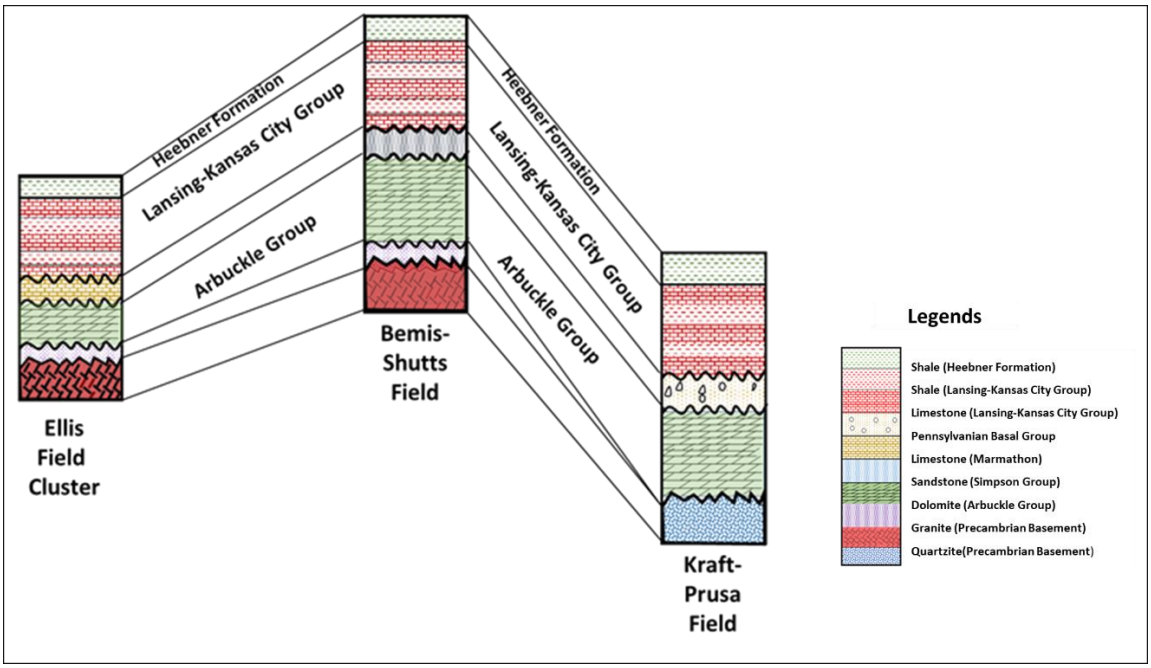

Figure 12: Succession of sedimentary layers in the three fields of the study location. Note: The stratigraphic thicknesses are not drawn to scale.

6.3.1 Maps of the Bemis-Shutts field

Four contour maps are generated from formation tops data from wells in the Bemis-Shutts field. The formation tops contoured are: 1) the Arbuckle, 2) the Simpson, 3) the Lansing-Kansas City, and 4) the Heebner. The map of the Arbuckle (Figure 13A) shows two structural highs similar to anticlinal features. On Figure 13A two structural highs are highlighted with yellow polygons (number 1 and number 2). The structural high 1 trends NE-SW and the structural high 2 trends N-S. The structural high 1 is not symmetrical. The slope of structural high 1 on the southeastern part is gentler, about 4 m / km (22 ft. / mile) (< 15 m / km or 50 ft./ mile) and the northeastern part is steeper, about 18 m / km (70 ft. / mile). The structural high 2 is almost symmetrical and shows an average gentle slope of about 7 m / km (35 ft. / mile). A channel-like feature is also observed in the Bemis-Shutts field which is outlined on Figure 13A.

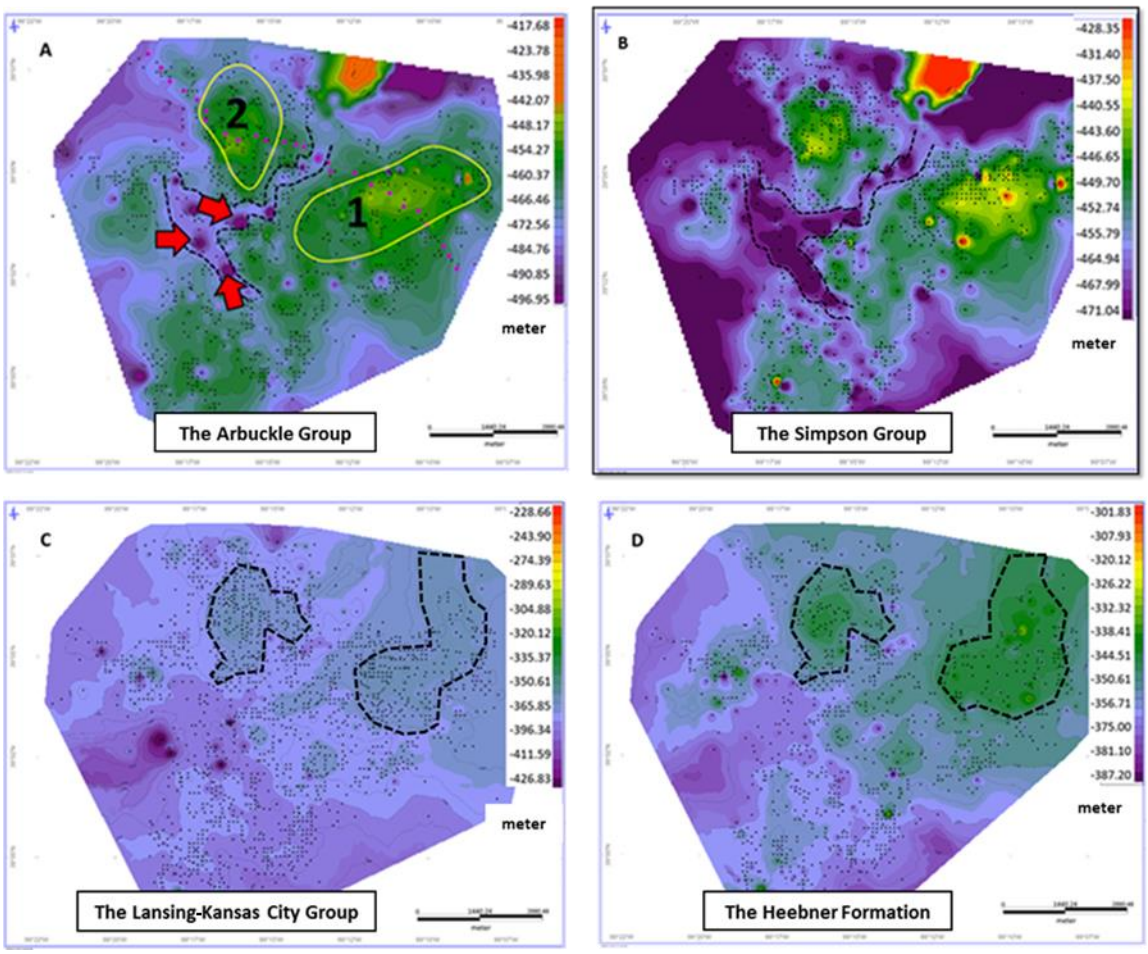

Figure 13: Contour maps of formations in the Bemis-Shutts field. A) Top of the Arbuckle. The map shows two structural highs and a channel-like low with circular features (indicated by arrows) that are possible karst features. B) Top of the Simpson. The map shows two main structural highs. C) Top of the Lansing-Kansas City. The map shows flat broad fold-like features on the northeastern corner. D) Top of the Heebner. The map shows similar features to the Lansing-Kansas City Group features over the Bemis-Shutts field. The dots show well locations.

The first part of this channel-like feature between the two structural highs discussed earlier (structural features 1 and 2 in Figure 13A), trends NE-SW. To the southwest of these two structural highs, the second part of the channel-like feature is outlined, which trends NW-SE. Within the channel-like feature, several circular features are also observed. The observed circular features are comparatively deeper than the surface of the channel-like feature. These features are possible karst features known to be present in the Arbuckle Group (Wilson et al., 1991). Rocks of the Arbuckle Group and

associated sedimentary features generally have relatively very low magnetic content, which make the structures unidentifiable in magnetic survey maps. Therefore, channel-like and karst features are not observed on the derivative filter maps. On the VDR map (Figure 7), NW-SE and NE-SW trending basement lineaments are observed at the Bemis-Shutts field. Similar structural trends on the basement and the structures (e.g., channel-like feature) in the sedimentary layer (e.g., the Arbuckle Group) suggest basement structural influence.

The contour map of the Simpson Group (Figure 13B) also shows two structural highs, and a channel-like feature similar to the structures observed in the Arbuckle Group. The Simpson Group directly overlay the Arbuckle Group where it is available. Similar structural trends and the presence of similar structural elements (e.g., structural highs, channel-like feature) to those observed in the Arbuckle Group, suggest that the structures in the Simpson Group are similarly influenced by basement structures.

The contour map of the Lansing-Kansas City Group (Figure 13C) shows a broad flat-topped feature on the northeast corner of the Bemis-Shutts field. Another structurally high feature is observed on the north-central portion. Compared to the structural highs observed in the Arbuckle and the Simpson Group, the highs in the Lansing-Kansas City Group are broader, less steep and flat-topped, indicating a change in deformational processes.

The pre-Pennsylvanian erosion not only eroded Mississippian sedimentary layers but also affected the pre-Mississippian sedimentary layers such as the Arbuckle Group and the Simpson Group. In addition, the tectonic activities during the Mississippian and Pennsylvanian period also deformed the pre-Mississippian sedimentary layers (Jewett

and Merriam, 1959; Merriam, 1963). Therefore, the structures in the Lansing-Kansas City Group do not mimic the structures of the underlying sedimentary strata (notably the Arbuckle and the Simpson Groups) that show basement structural influence. These differences suggest that structures in the Lansing-Kansas City Group are not significantly influenced by basement structures, or to the same extent, like the Arbuckle and the Simpson Group.

The Heebner Formation directly overlay the Lansing-Kansas City Group. The contour map of the Heebner Formation (Figure 13D) shows similar structural trends to the structures observed in the Lansing-Kansas City Group. Similar shape and trend of structural features suggest that structures in the Heebner Formation are influenced by the underlying topography of the Lansing-Kansas City Group.

6.3.2. Maps of the Ellis Cluster Field

Three contour maps are generated from formation tops data obtained from wells in the Ellis Cluster field. The formation tops contoured are: 1) the Arbuckle, 2) the Lansing-Kansas City, and 3) the Heebner.

The contour map of the Arbuckle Group shows two structural highs (anticlinal features) trending NW-SE (Figure 14A). The slope of both anticlines are very gentle about 4.5 m / km (24 ft. / mile) and are almost symmetrical. These anticlinal features appear to be influenced by the Rush rib, because the Ellis Cluster field is approximately located on the northeastern part of the CKU above the Rush rib (Koster, 1935). The VDR and TDR maps (Figures 7 and 8) show a set of NW-SE trending lineaments on the southwestern corner of the study area which are possible basement faults bounding the

Rush rib. According to previous study (Koster, 1935), these basement faults were reactivated during the Mississippian due to tectonic activities which developed secondary structures (e.g., Rush rib, Russell rib) along with the CKU.

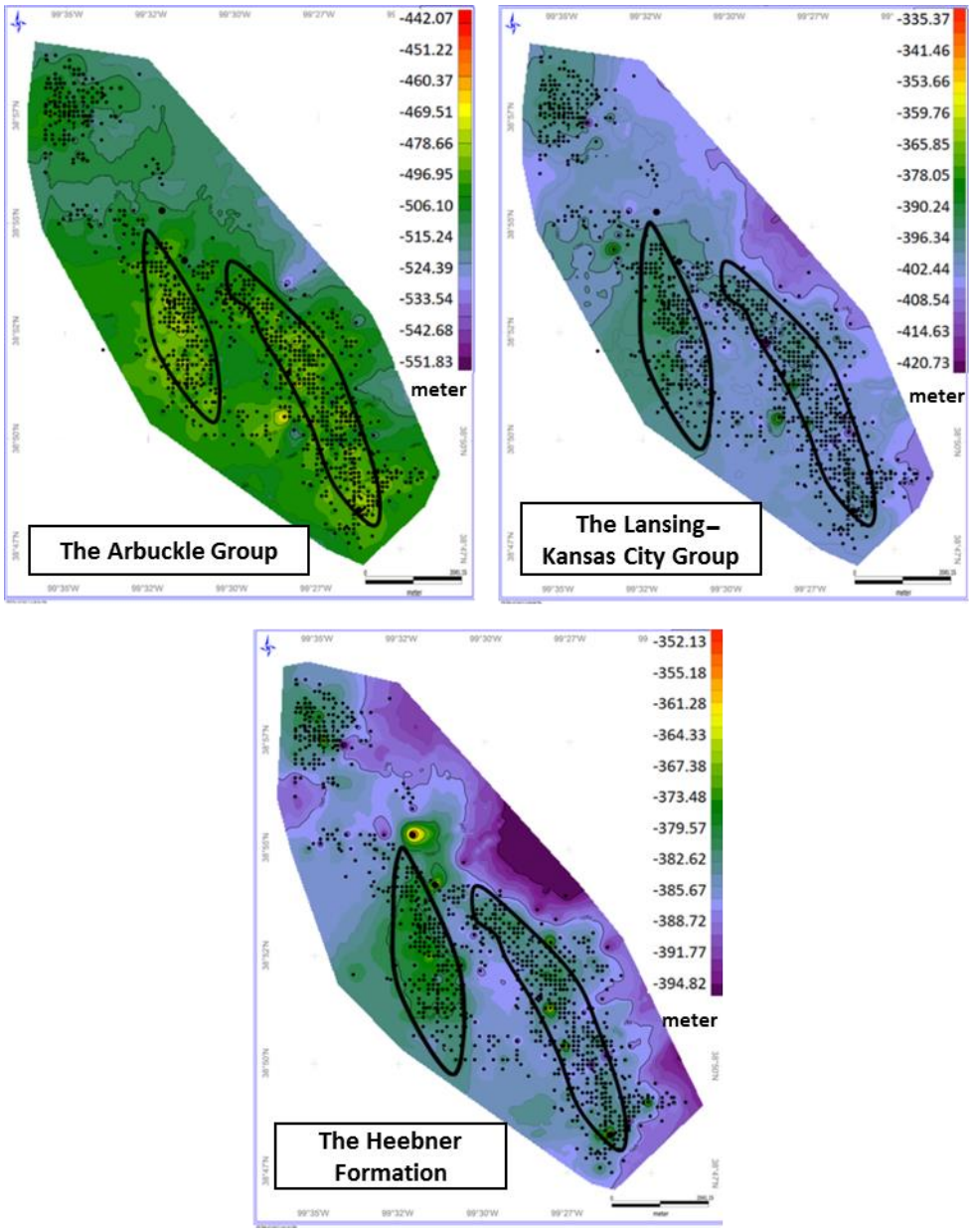

Figure 14: Contour maps of formations in the Ellis Cluster field. A) Top of the Arbuckle. B) Top of the Lansing-Kansas City. C) Top of the Heebner. The outlined areas show structural highs. The Heebner map shows structures similar to the Lansing-Kansas City Group. The dots show well locations.

In addition to the deformation, the Arbuckle beds were truncated as result of tectonic events occurred in the Mississippian (Ballard and Reinschmidt, 1995). Underlying basement structures (Rush rib and faults bounding it) and the location of anticlinal features observed in the Arbuckle Group, suggest basement structural influence on the pre-Mississippian sedimentary layers (e.g., the Arbuckle Group).

In the Ellis Cluster field, the pre-Pennsylvanian erosion not only eroded Mississippian sedimentary layers but also affected the pre-Mississippian sedimentary layers such as the Arbuckle and the Simpson Group (Merriam, 1963). As a result, the Simpson Group in the Ellis Cluster field is completely absent, and the Lansing-Kansas City Group directly overlays the extensively eroded surface of the Arbuckle Group in most places. The contour map of Lansing-Kansas City Group (Figure 14B) shows two structural highs (anticlinal features) trending NW-SE. Observed structural highs in the Lansing-Kansas City Group show similar structural trend and shape to the underlying structures observed in the Arbuckle. The similarities between structures in the Lansing-Kansas City and the Arbuckle Group suggest a direct influence of the underlying topography of the Arbuckle Group which is a continuation of basement influence.

The Heebner Formation directly overlay the Lansing-Kansas City Group all over the Ellis Cluster field. The formation tops contour map of the Heebner Formation (Figure 14C) shows similar structures to those observed in the Lansing-Kansas City Group. This similarity suggests an influence of the underlying topography of Lansing-Kansas City Group and shows direct influence of the basement structures.

6.3.3. Maps of the Kraft-Prusa Field

Three contour maps are generated from formation tops data from wells in the Kraft-Prusa field. The formation tops contoured are:1) the Arbuckle, 2) the Lansing-Kansas City, and 3) the Heebner.

The formation tops contour map (Figure 15A) of the Arbuckle Group shows six highs. Two of the most prominent highs in the northwest part of the field is-aligned with the underlying NE-SW trend. Although, previous studies (Walter, 1946; 1958) identified six structural highs or basement hills underlying the Arbuckle Group in the Kraft-Prusa field, none of these highs are identified on the derivative maps. However, the NE-SW trending basement lineaments are observed on the derivative maps. The observations from derivative and contour maps suggest that, the basement structural highs are aligned in a NE-SW direction and have influenced the observed structural highs in the Arbuckle Group .

Rocks of the Lansing-Kansas City Group directly overlay the Arbuckle Group in the Kraft-Prusa field. The contour map of the Lansing-Kansas City Group (Figure 15B) shows two broad and gently sloping on the northwest part of the Kraft-Prusa field. These highs overlay the structural highs described in the Arbuckle Group in the previous section (outlined polygon in Figure 15B). Similar patterns and locations of structural highs on the Lansing-Kansas City Group also suggest basement structural influence.

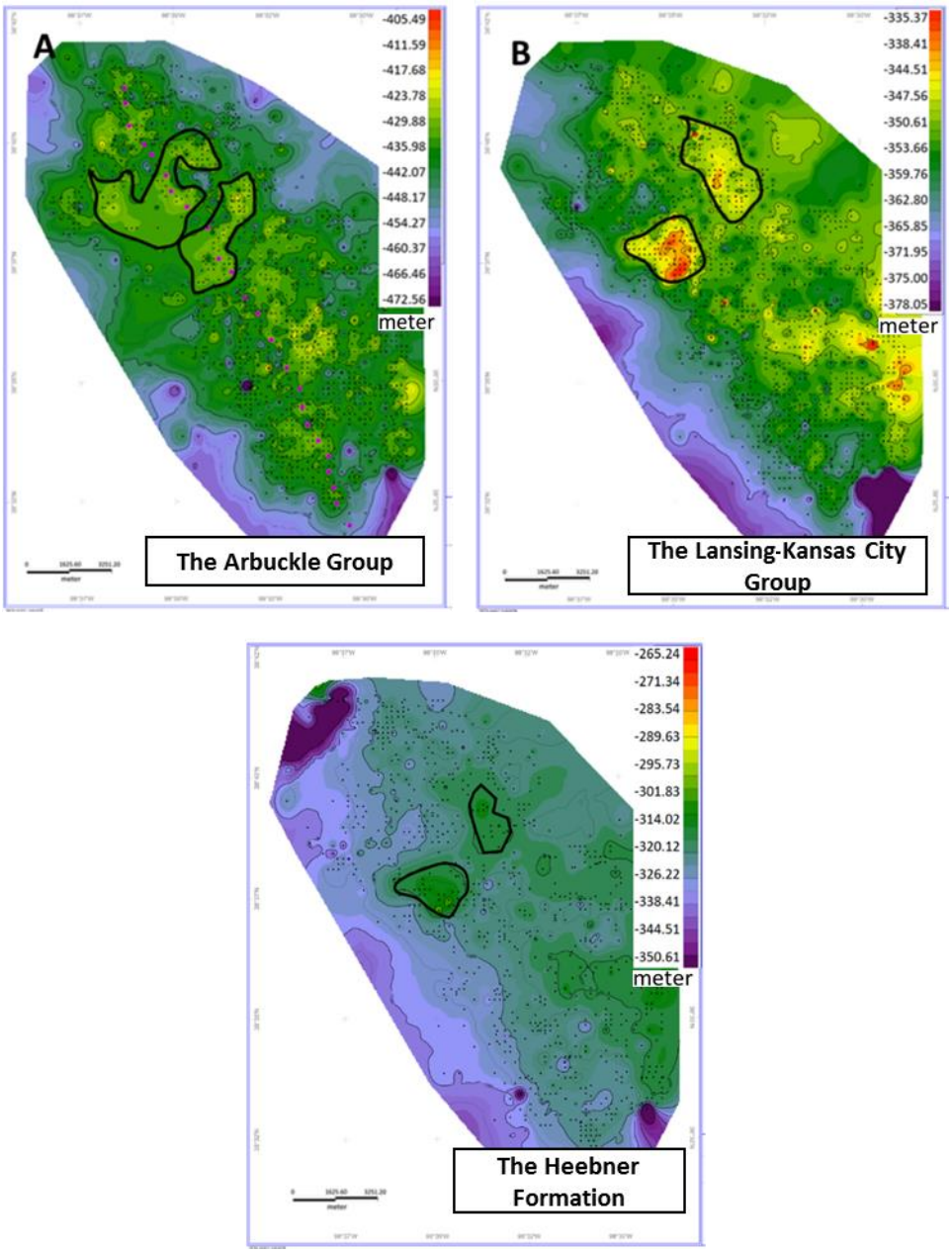

Figure 15: Contour maps of formations in the Kraft-Prusa field. A) Top of the Arbuckle. B) Top of the Lansing-Kansas City. C) Top of the Heebner. Outlined areas show structural highs. The dots show well locations

On the contour map of the Heebner Formation (Figure 15C) two structural highs are observed, similar to the structural features on the Lansing-Kansas City Group. These observations suggest similar structural influence of underlying structures on the Heebner Formation.

6.3.4. Summary

Basement structural influence on the direct overlaying formations (e.g., the Arbuckle Group) is observed in all three fields. The basement structural influence observed in the Bemis-Shutts and in the Ellis Cluster field are almost similar. In both cases, it is observed that anticlinal features are bounded by faults. In the Kraft-Prusa field, most of the observed structural highs are aligned in NE-SW direction and the influence of the basement structural highs on the overlaying strata is noticeable. Structural features on the Lansing-Kansas City Group and on the Heebner Formation are not significantly influenced by the basement structures. Instead, structural features of these two sedimentary strata (e.g., the Lansing-Kansas City Group and the Heeber Formation) overlaying the Arbuckle Group are observed to be influenced by the underlying topography and structural features.

7. CONCLUSION

The interpretation of aeromagnetic data of the study location show two distinct orientations of structures in the basement of the study area. These are: (1) NE-SW trending lineaments, and (2) NW-SE trending lineaments. NE-SW trending lineaments associated with the MRS are observed to truncate the NW-SE trending lineaments in the southeastern part of the CKU. Two basement structural highs are identified in this study which are known as the Russell and the Rush rib.

The depths to basement were estimated from the aeromagnetic data using the Source Parameter Imaging (SPI) method and from contour maps of formation tops. The estimated depths from the SPI vary between -112 m (-368 ft.) and -1187 m (-4232 ft.) and the depths from the basement tops contour map vary between -441 m (-1445 ft.) and -627 m (-2057 ft.) subsea. The accuracy of estimated depths from the SPI compared with the actual depths to basement from the well log data is within -22% and 10%.

The influence of underlying basement topography and basement structures on the pre-Mississippian strata (the Arbuckle Group and the Simpson Group), were observed in all three fields. Structural features in the pre-Mississippian strata are mostly anticlinal features, which appeared to be influenced by faults bounding the Russell and Rush ribs. On the other hand, the structural features in the Kraft-Prusa field are more influenced by basement topographic high or basement hills.

Structures in the Arbuckle Group influenced post-Mississippian sedimentary layers (the Lansing-Kansas City Group and the Heebner Formation) overlaying it. The similarities between the trends and shape of structural features in the Lansing-Kansas City Group and the Heebner Formation are notable in the Ellis Cluster field and the

Kraft-Prusa field. However, no significant influence of underlying structures on the Lansing-Kansas City Group and the Heebner Formation in the Bemis-Shutts field was not observed.

8. REFERENCES

Ali, H., S. Reed, E. Atekwana, and E. Atekwana, 2013, Magnetic susceptibility is associated with oil-bearing intervals in an oil field, north-central Kansas: SEG Technical Program Expanded Abstracts 2013, 581-586.

Allek, K., and M. Hamoudi, 2008, Regional-scale aeromagnetic survey of the south-west of Algeria: a tool for area selection for diamond exploration: Journal of African Earth Sciences, 50, 67-68.

Adler, F. J., 1971, Future petroleum provinces of the United States-their geology and potential: American Association of Petroleum Geologists Memoir 15, 985-1,120.

Baars, D. L., 1995, Basement tectonic configuration in Kansas: Kansas Geological Survey Bulletin, 237, 7-9.

Baars, D. L., and W. L. Watney, 1991, Paleotectonic control of reservoir facies: Kansas Geological Survey Bulletin, 233, 253-262.

Ballard, D.W., and D. D. Reinschmid, 1995, Roland SE Field, Rush County, Kansas: Kansas Geological Survey Bulletin, 237, 99-102

Bickford, M. E., K. L. Harrower, W.J. Hoppe, B.K. Nelson, R. l. Nusbaum, and J. J. Thomas, 1981, Rb-Sr and U-Pb geochronology and distribution of rock types in the Precambrian basement of Missouri and Kansas: Geological Society of America Bulletin, 92(6), 323-341.

Bickford, M. E., W. R. Van, and I. Zietz, 1986, Proterozoic history of the midcontinent region of North America: Geology, 14(6), 492-496.

Cansler, J. R., and T. R. Carr, 2002, Paleogeomorphology of the sub-Pennsylvanian unconformity of the Arbuckle Group (Cambrian–Lower Ordovician): Kansas Geological Survey Open-File Report 2001-55, 3.

Cole, V., 1975, Subsurface Ordovician-Cambrian Rocks in Kansas: Kansas Geological Survey, Subsurface Geology Series 2.

Cooper, G. R. J., and D. R. Cowan, 2004, Filtering using variable order vertical derivatives: Computers & Geosciences, 30(5), 455-459.

Franseen, E. K., 1994, Facies and porosity relationships of Arbuckle strata: Initial observations from two cores. Rice and Rush counties, Kansas: Kansas Geological Survey, Open-file Report, 53, 34.

Franseen, E. K., A. P. Byrnes, J. R. Cansler, and T. Carr, 2004, Geology of Kansas: Arbuckle Group: Current Research in Earth Sciences Bulletin A, 250, part 2.

Gabtni, H., C. Jallouli, K. L. Mickus, M. Dhaoui, M. M. Turki, M. Jaffal, and P. Keating, 2012, Basement structure of southern Tunisia as determined from the analysis of gravity data: implications for petroleum exploration: Petroleum Geoscience, 18(2), 143-152.

Gay, S. P., 1995, Basement control of selected oil and gas fields in Kansas as determined by detailed residual aeromagnetic data: Kansas Geological Survey Bulletin, 237, 10-16.

Gerhard, L. C., 2004, A new look at an old petroleum province. Lawrence, KS: Kansas Geological Survey.

Grant, F. S., and J. Dodds. "MAGMAP FFT processing system development notes: Paterson Grant and Watson Limited." (1972).

Gunn, P. J., 1975, Linear transformations of gravity and magnetic fields. Geophysical Prospecting, 23(2), 300-312.

Henkel, H., W. U. Reimold and C. Koeberl, 2002, Magnetic and gravity model of the Morokweng impact structure: Journal of Applied Geophysics, 49.3, 129-147.

Jewett, J. M., 1951, Geologic structures in Kansas: Kansas Geological Survey Bulletin, 90, part 6.

Jewett, J. M., and D. F. Merriam, 1959, Geologic framework of Kansas; a review for geophysicists. In Symposium on geophysics in Kansas: Kansas Geological Survey Bulletin, 137, 9-52.

Kinabo, B. D., E. A. Atekwana, J. P. Hogan, M. P. Modisi, D. D. Wheaton, and A. B. Kampunzu, 2007, Early structural development of the Okavango rift zone, NW Botswana: Journal of African Earth Sciences, 48(2), 125-136.

Kluth, C. F., and P. J. Coney, 1981, Plate tectonics of the ancestral Rocky Mountains: Geology, 9(1), 10-15.

Koester, E. A., 1935, Geology of central Kansas uplift: American Association of Petroleum Geologist Bulletin, 19(10), 1405-1426.

MacLeod, I. N., K. Jones, and T.F. Dai, 1993, 3-D analytic signal in the interpretation of total magnetic field data at low magnetic latitudes: Exploration Geophysics, 24(3/4), 679-688.

Merriam, D. F., 1963, The geologic history of Kansas: Kansas Geological Survey Bulletin, 162, 317.

Merriam, D. F., 1955, Structural patterns in western Kansas: Kansas Geological Society Annual Field Conference, 18, 80-87.

Miller, H. G., and V. Singh, 1994, Potential field tilt- a new concept for location of potential field sources: Journal of Applied Geophysics, 32(2-3), 213-217.

Miller, H. G., and V. Singh, 1994, Semi quantitative techniques for the removal of directional trends from potential field data: Journal of Applied Geophysics, 32, 199-211.

Nabighian, M. N., 1972, The analytic signal of two-dimensional magnetic bodies with polygonal cross-section: Its properties and use for automated anomaly interpretation: Geophysics, 37(3), 507-517.

Newell, K. D., W. L. Watney, D. W. Steeples, R.W. Knapp, and S. W. Cheng, 1989, Suitability of high-resolution seismic method to identifying petroleum reservoirs in Kansas: A geological perspective: Kansas Geological Survey Bulletin, 226, 9-30.

Newell, K.D., W. L. Watney, S. W. L. Cheng, and R. L. Brownrigg, 1987, Stratigraphic and spatial distribution of oil and gas production in Kansas: Kansas Geological Survey, Subsurface Geology Series, 9, 86.

Peel, F., C. J. Travis, and J. R. Hossack, 1995, Genetic structural provinces and salt tectonics of the Cenozoic offshore US Gulf of Mexico: a preliminary analysis: American Association of Petroleum Geologist, Memoir. 65, 153 – 175.

Pilkington, M., W. F. Miles, G. M. Ross, and W. R. Roest, 2000, Potential-field signatures of buried Precambrian basement in the Western Canada Sedimentary Basin: Canadian Journal of Earth Sciences, 37(11), 1453-1471.

Rascoe, J., and F. J. Adler, 1983, Permo-Carboniferous hydrocarbon accumulations, mid-continent, USA: American Association of Petroleum Geologist Bulletin, 67(6), 979-1001.

Reeves, C., 2005, Aeromagnetic Survey: Principle, Practice, and Interpretation: Delft, Netherland. Geosoft.

Robinson, E. S., 1988, Basic exploration geophysics: Somerset, NJ. John Wiley and Sons, Inc.

Roest, W. R., J. Verhoef, and M. Pilkington, 1992, Magnetic interpretation using the 3-D analytic signal: Geophysics, 57(1), 116-125.

Salem, A., S. Williams, D. Fairhead, R. Smith, and D. Ravat, 2007, Interpretation of magnetic data using tilt-angle derivatives: Geophysics, 73(1), L1-L10.

Sloss, L. L., 1963, Sequence in the cratonic interior, Geological Society of America Bulletin, 74, 93-113.

Smith, R. S., J. B. Thurston, T.F. Dai, & I. N. MacLeod, 1998, ISPITM—the improved source parameter imaging method: Geophysical Prospecting, 46(2), 141-151.

Smith, R. S. and A. Salem, 2005, Imaging depth, structure, and susceptibility from magnetic data: The advanced source-parameter imaging method: Geophysics, 70(4), L31-L38.

Thurston, J. B. and R. S. Smith, 1997, Automatic conversion of magnetic data to depth, dip, and susceptibility contrast using the SPI (TM) method: Geophysics, 62(3), 807-813.

Van Schmus, W. R., and W. J. Hinze, 1985, The midcontinent rift system: Annual Review of Earth and Planetary Sciences, 13(1), 345-383.

Van Schmus, W. R., M. E. Bickford, and I. Zietz, 1987, Early and Middle Proterozoic provinces in the central United States: American Geophysical Union Geodynamic Series, 17, 43-68.

Verduzco, B., J. D. Fairhead, C. M. Green, and C. Mackenzie, 2004, New insights into magnetic derivatives for structural mapping: The Leading Edge, 23(2), 116-119.

Walters, R. F., 1946, Buried pre-Cambrian hills in northeastern Barton County, central Kansas: American Association Petroleum Geologist Bulletin, 30(5), 660-710.

Walters, R. F., 1958, Differential entrapment of oil and gas in Arbuckle dolomite of central Kansas: American Association Petroleum Geologist Bulletin, 42(9), 2133-2173.

Watney, W. L., 1980, Cyclic sedimentation of the Lansing-Kansas City groups in northwestern Kansas and southwestern Nebraska: Kansas Geological Survey Bulletin, 200, 72.

Watney, W. L., E. K. Franseen, A. P. Byrnes, and S. E. Nissen, 2008, Evaluating structural controls on the formation and properties of Carboniferous carbonate reservoirs in the northern Midcontinent, U.S.A., in J. Lukasik and J. A. Simo, eds., Controls on carbonate platform and reef development: SEPM Special Publication, 89, 21.

Williams, D. L. and C. A. Finn, 1985, Analysis of gravity data in volcanic terranes and gravity anomalies and sub-volcanic intrusions Cascade Range, USA and at other selected volcanoes, in Utility of Gravity and Magnetic Maps, edited by W. Hinze: Society of Exploration Geophysicists, Tulsa, Oklahoma, 341-374.

Wilson, J. L., R. D. Fritz, and P. L., Medlock, 1991, The Arbuckle Group: Relationship of core and outcrop analyses to cyclic stratigraphy and correlation: Oklahoma Geological Survey Special Publication, 91-3.

Xia, J., R. Miller, and D. Adkins-Heljeson, 2000, Potential-field Database at the Kansas Geological Survey, accessed on 24 April 2017, http://www.kgs.ku.edu/Geophysics/OFR/2000/6/index.html

Xia, J., D. R. Sprowl, and D. W. Steeples, 1996, A model of Precambrian geology of Kansas derived from gravity and magnetic data: Computers & Geosciences, 22(8), 883-895.

Yarger, H. L., 1982, Regional interpretation of Kansas aeromagnetic data: Kansas Geological Survey Open-File Report, 82-22, 1 (3), 101.

Yarger, H. L., 1989, Major magnetic features in Kansas and their possible geologic significance: Kansas Geological Survey, Bulletin, 226, 197-213.